# Neutron and beta imaging with Micromegas detectors with optical readout

## MPGD 2022 – 15/12/2022

A. Cools, E. Ferrer-Ribas, T. Papaevangelou, E. C. Pollacco, T. Benoit, D. Desforge
(Université Paris-Saclay, CEA, IRFU)
F.M. Brunbauer, L. Ropelewski, E. Oliveri (CERN)
F. Beau, L. Devel, C. Malgorn (Université Paris-Saclay, CEA, Institut Joliot)
F.J. Iguaz-Gutierrez (Soleil Synchrotron)
A. Sari (Université Paris-Saclay, CEA, List)

מכון ויצמן למדע
WEIZMANN INSTITUTE OF SCIENCE

# CONTEXT

## LIGHT PRODUCTION MECHANISMS

## LIGHT DETECTION DEVICES

# DETECTOR CHARACTERIZATION WITH X-RAY SOURCES

# APPLICATIONS

## B-IMAGING

## PRELIMINARY RESULTS WITH TRITIUM SAMPLES

## NEUTRON RADIOGRAPHY

## PRELIMINARY RESULTS WITH A NEUTRON SOURCE

# CONCLUSION AND PERSPECTIVES

# CONTEXT

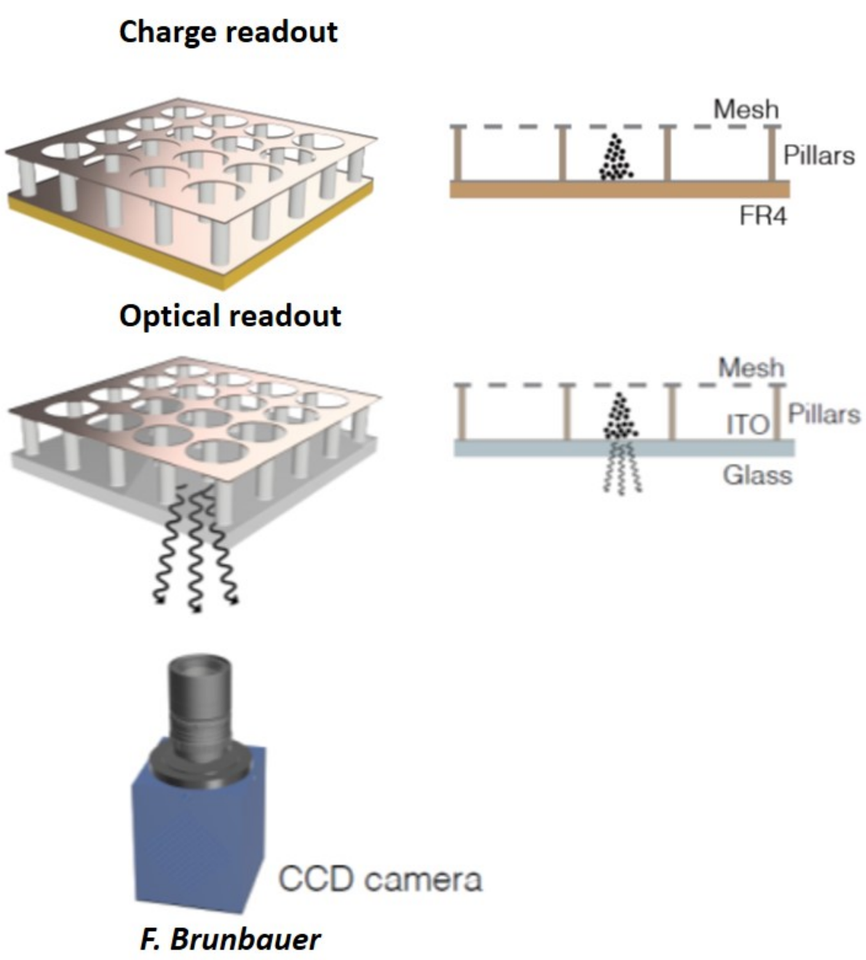


## Advantages:

- 2D pixelized readout of high granula
- Megapixel resolution from commerc
- Integrated imaging approach

## Applications:

- Real-time neutron imager
- β imager for sub-becquerel activity r

Nuclear Inst. and Methods in Physics Research, A 955 (2020) 163320

Contents lists available at ScienceDirect

Nuclear Inst. and Methods in Physics Research, A

journal homepage: www.elsevier.com/locate/nima

Radiation imaging with glass Micromegas

F.M. Brunbauer [a], D. Desforge [b], E. Ferrer-Ribas [b], F.J. Iguaz [b], B. Mehl [a], R. De Oliveira [a], E. Oliveri [a], T. Papaevangelou [b], O. Pizzirusso [a], E.C. Pollacco [b,*], F. Resnati [a], L. Ropelewski [a], L. Segui [b], M. van Stenis [a]

[a] European Organization for Nuclear Research (CERN), CH-1211 Geneve 23, Switzerland
[b] IRFU, CEA, Université Paris-Saclay, F-91191 Gif-sur-Yvette, France

ARTICLE INFO

Keywords:
Radiation imaging
Optical readout
MPGD
Micromegas
Glass Micromegas
Scintillation
ITO

ABSTRACT

Optically recording scintillation light emitted by MicroPattern Gaseous Detectors (MPGDs) with imaging sensors is a versatile and performant readout modality taking advantage of modern high granularity imaging sensors. To allow scintillation light readout of a detector based on MicroMesh Gaseous Structure (Micromegas) technology, we have integrated a Micromegas on a glass substrate with a transparent anode. In addition to optical detection of scintillation light emitted during electron avalanche multiplication between the micromesh and the anode, this setup also achieves a good energy resolution. A glass Micromegas detector was operated in an $Ar/CF_4$ gas mixture and showed a response comparable to conventional Micromegas detectors. The spectrum of the emitted scintillation light was recorded and shown to be equivalent to the one obtained with other gaseous detectors in the same gas mixture. Optically read out images were recorded with CCD cameras and integrated X-ray radiographic imaging with good spatial resolution was demonstrated. A spatial resolution of 440 µm (10% MTF) was found. Single X-ray photon detection with a high-sensitivity camera was achieved, which potentially permits energy-resolved X-ray fluorescence imaging.

1. Introduction

Optical readout of MicroPattern Gaseous Detectors (MPGDs) takes advantage of combining the high gain factors achievable by MPGD technologies with the high granularity pixel readout permitted by modern imaging sensors. This allows for the realisation of radiation detectors with spatial resolution and sensitivity to a wide range of radiation ranging from Minimum Ionising Particles (MIPs) to low-energy X-rays, as well as highly ionising radiation such as alpha particles. Detector concepts based on optically read out MPGD-based detectors have been previously developed for applications such as radiation imaging [1,2], 3D track reconstruction in optically read out Time Projection Chambers (TPCs) [3,4] or dose imaging in hadron therapy [5,6]. Previous MPGD-based detector concepts employing optical readout with imaging sensors were predominantly based on Gaseous Electron Multipliers (GEMs), a variety of MPGDs consisting of perforated multilayer foils. This geometry makes GEMs well-suited for optical readout as scintillation light emitted during electron avalanche multiplication can be easily recorded by a camera placed behind the detector. In contrast, most other MPGD technologies are integrated on substrates such as Printed Circuit Boards (PCBs) which are opaque and thus inhibit scintillation light recording. This is also true for MicroMesh Gaseous Structures (Micromegas), which employ a micro-mesh supported by insulating pillars to create a uniform amplification region with an electric field strength sufficient for electron avalanche amplification between the micro-mesh and an anode [7]. However, Micromegas are typically integrated on PCBs, which has previously inhibited the optical readout of such detectors.

We have developed a Micromegas detector on a glass substrate with a transparent anode made of Indium Tin Oxide (ITO) to enable the optical readout of Micromegas-based detectors. Thus it is possible to take advantage of the superior energy resolution reached by this MPGD technology as well as profit from the high spatial resolution and intuitive 2D imaging capabilities associated with optical readout with state-of-the-art imaging sensors.

This enables the readout of secondary scintillation light emitted during electron avalanche multiplication in the amplification gap between the micro-mesh and the anode. As with the optical readout of GEM-based detectors, the glass Micromegas were operated in an $Ar+CF_4$ gas mixture. Gas mixtures containing $CF_4$ feature wide scintillation light emission bands in the ultraviolet (UV) and visible (VIS) wavelength ranges [8], which are compatible with the wavelength-dependent quantum efficiency (QE) of common CCD and CMOS imaging sensors. Optical readout of GEM-based detectors operated in $Ar+CF_4$ gas mixtures has been reported and used for X-ray radiography [1,2] as well as 3D track reconstruction [3,4].

* Corresponding author.
E-mail address: emmanuel.pollacco@cea.fr (E.C. Pollacco).

https://doi.org/10.1016/j.nima.2019.163320
Received 1 October 2019; Received in revised form 17 December 2019; Accepted 18 December 2019
Available online 19 December 2019

# LIGHT PRODUCTION MECHANISMS

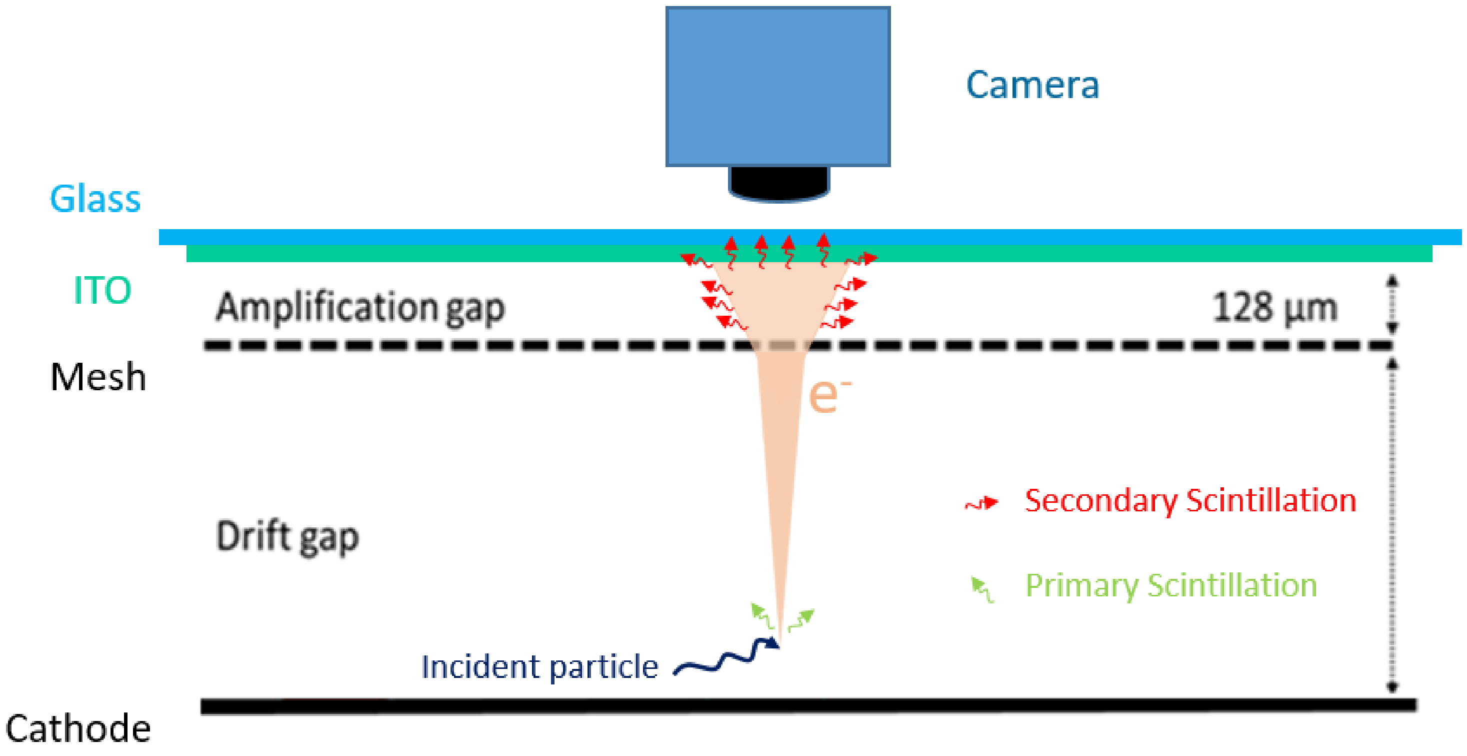


Gas mixture : $Ar/CF_4$

**Scintillation**

↓

**Fluorescence**

Prompt emission of photon after absorption of incident radiation. (1 ns to 1 µs)

| **Primary scintillation** | **Secondary scintillation** |
| --- | --- |
| Coming from the excitation of the gas due to incident particles. | Coming from avalanche amplification. |

# LIGHT DETECTION DEVICES

## Hamamatsu CMOS camera

ORCA®-Quest

### Readout noise

| | |
|---|---|
| Standard scan | 0.43 electrons rms |
| Ultra quiet scan | 0.27 electrons rms |

### Pixels

| Number | Size |
|---|---|
| 4096 x 2304 | 4.6 µm x 4.6 µm |

### Dark current

| Cooling | Sensor temperature | Dark current |
|---|---|---|
| Air | - 20 °C | 0.016 $e^-$ /pixels/s |

### Minimum exposure time

| Mode | Rate |
|---|---|
| Standard | 1 µs/frame |
| Ultra quiet | 100 ms/frame |

### Photon number resolving

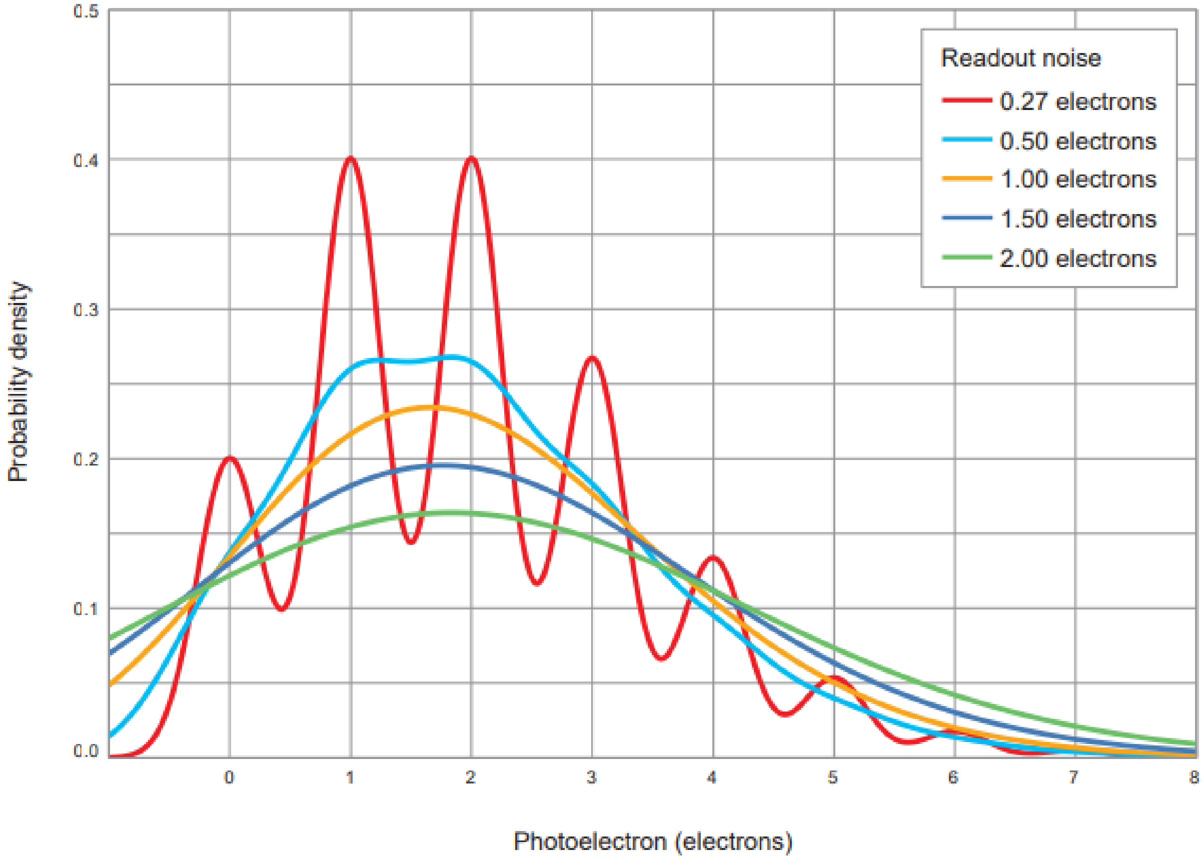

# LIGHT DETECTION

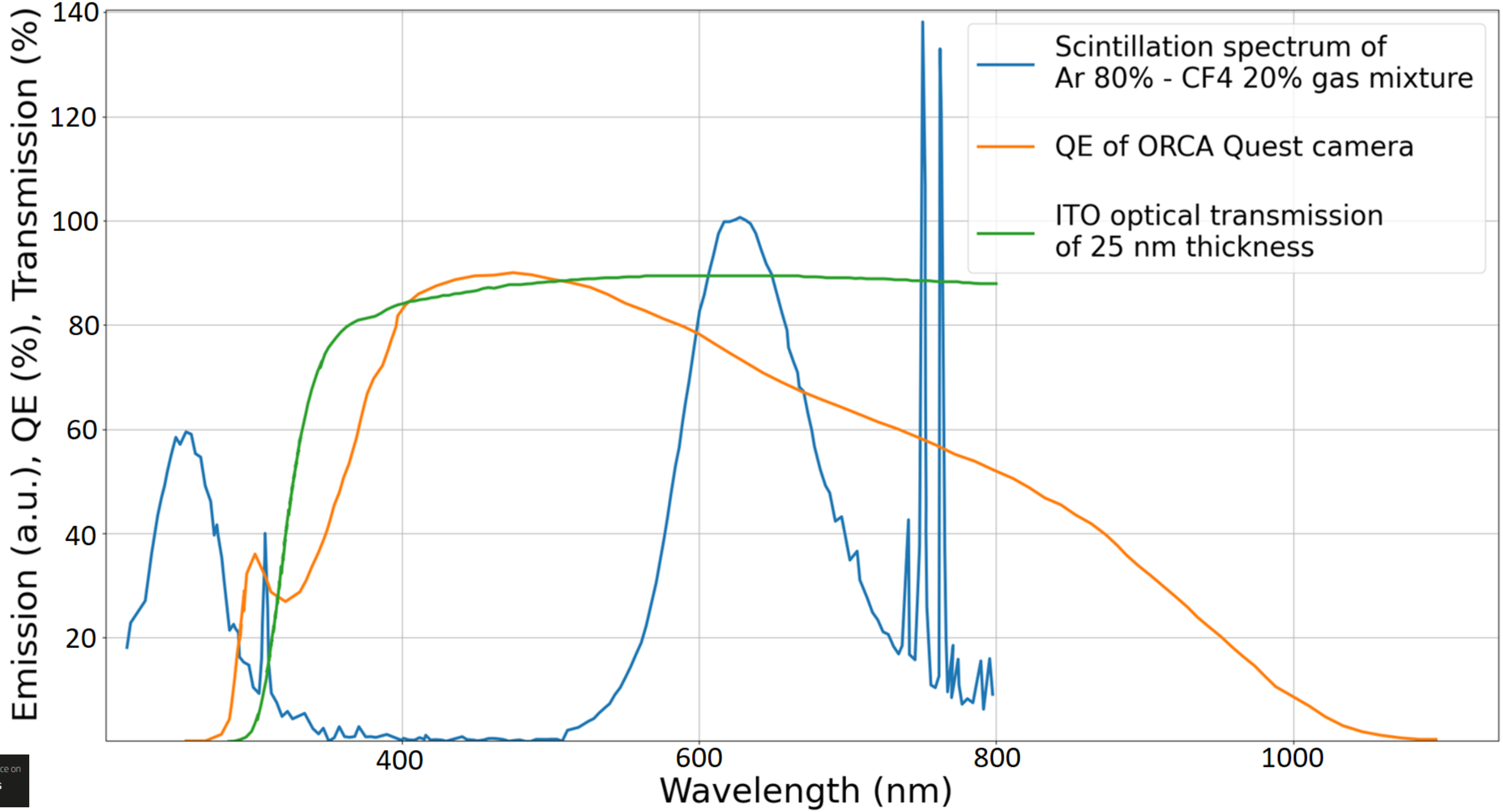

# DETECTOR CHARACTERIZATION WITH X-RAY SOURCES

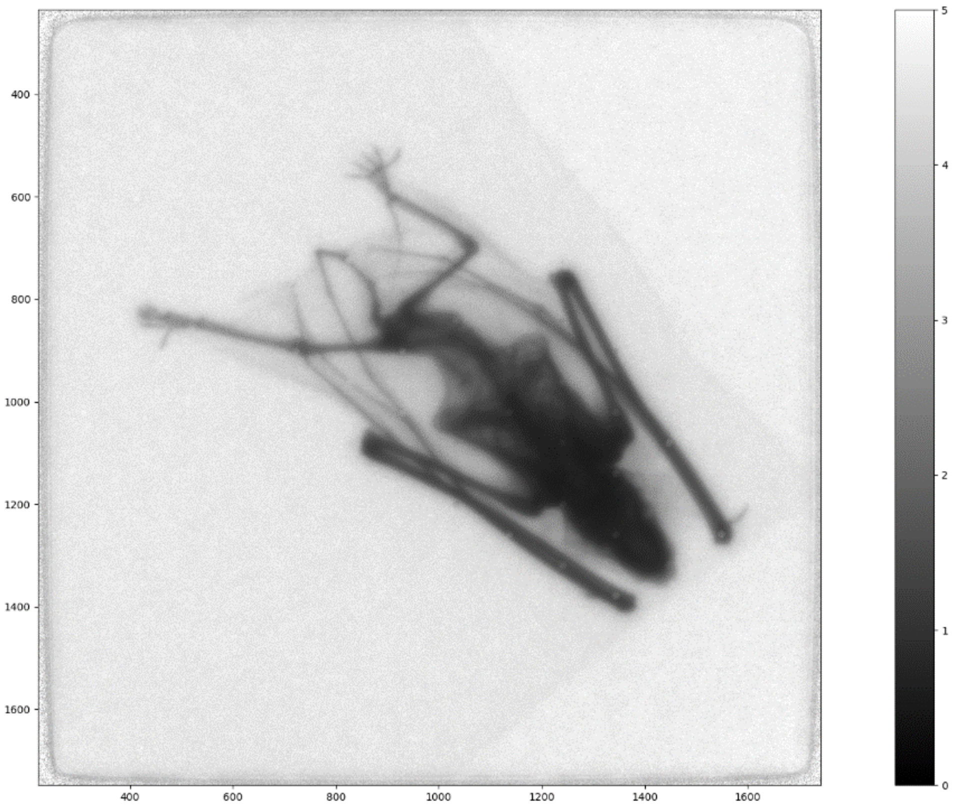


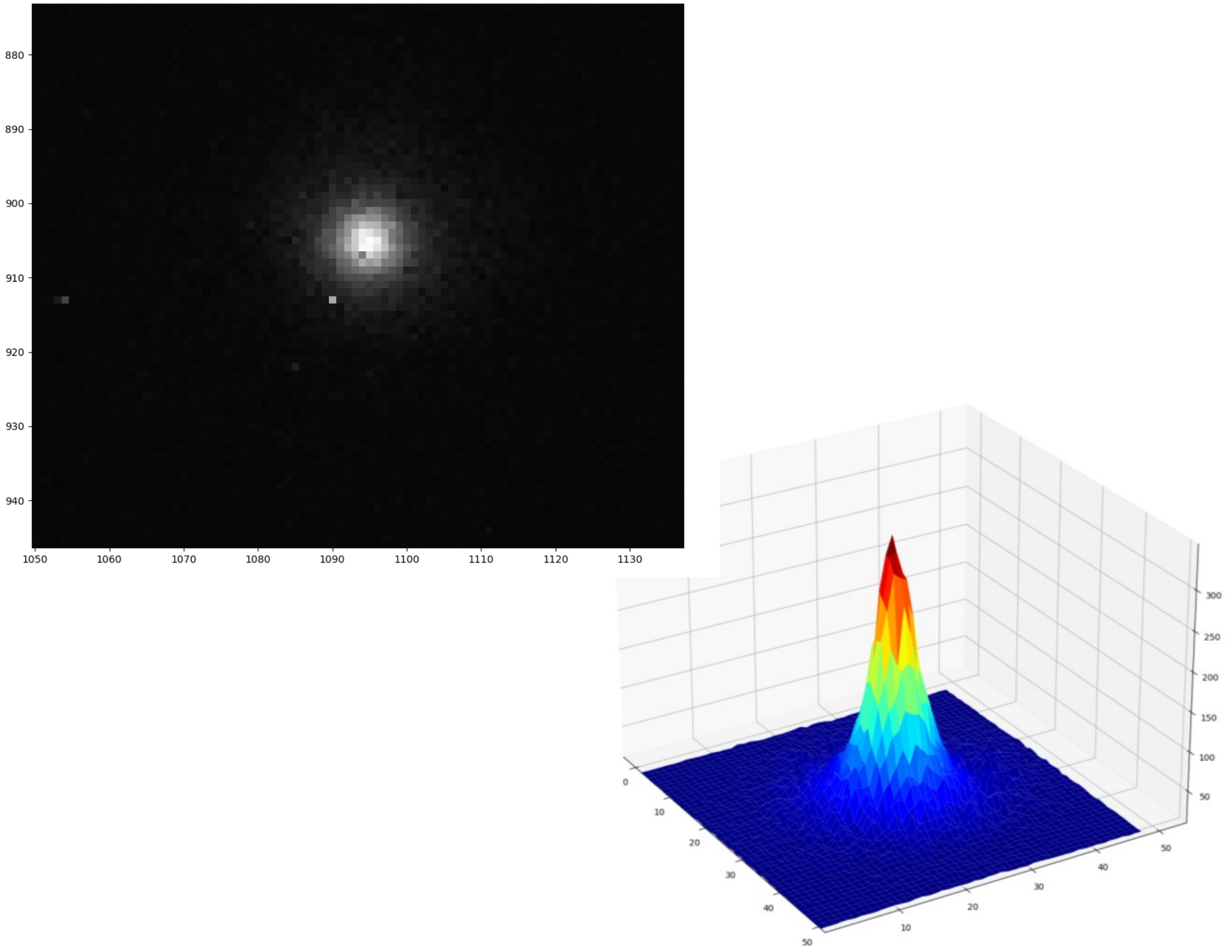

# DETECTOR CHARACTERIZATION WITH X-RAYS

*Experimental set-up for x-rays*

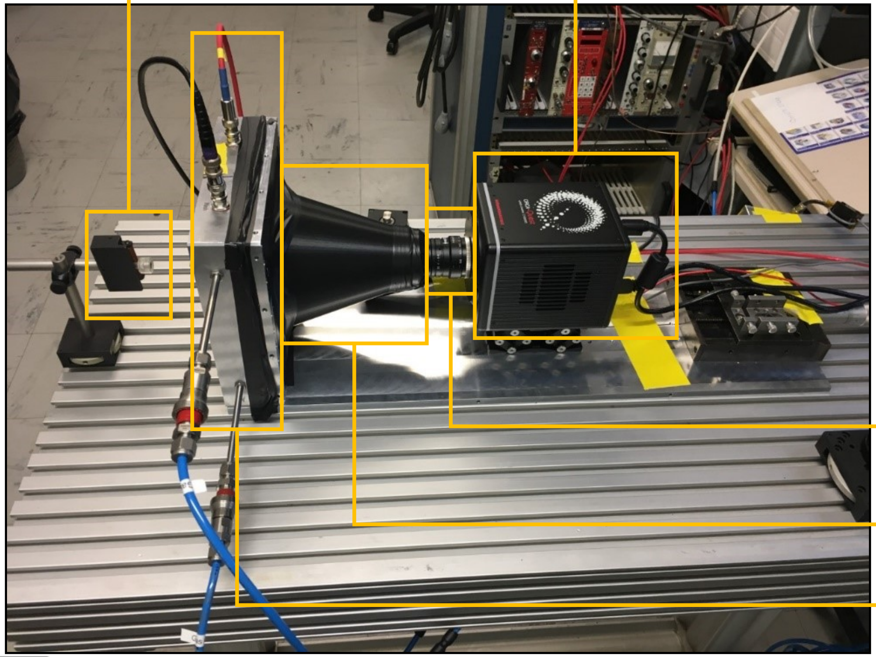


S. Aune, T. Benoit, M. Kebbiri

## Bulk on glass from CERN and IRFU

- Charge readout test in Argon+5%Iso:
  **gain** above **10$^4$** and **FWHM** reaches **16%**
- Coated glass with 150 nm of ITO (Indium Thin Oxide)
- Pillars with hexagonal pattern and large pitch (6 mm)

Charge readout spectrum in Ar/Iso 5%

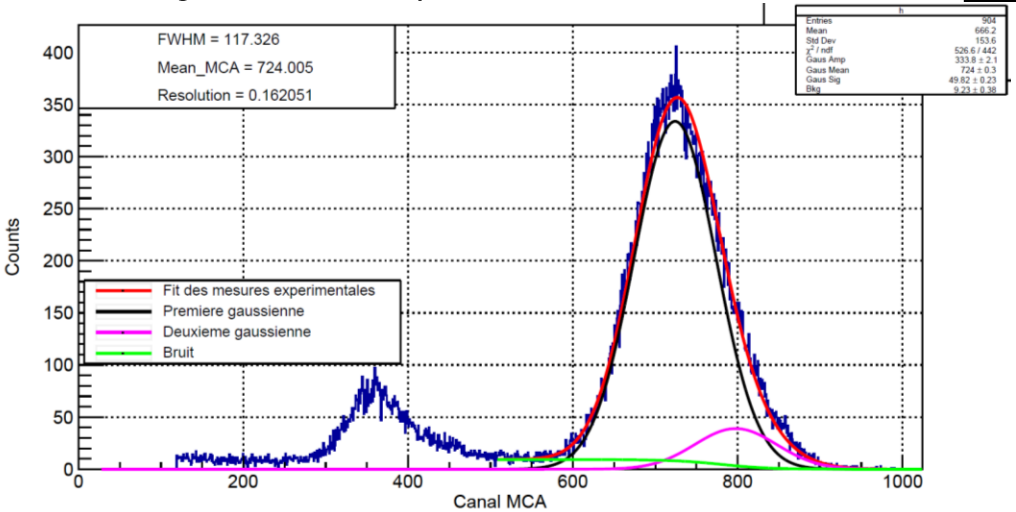


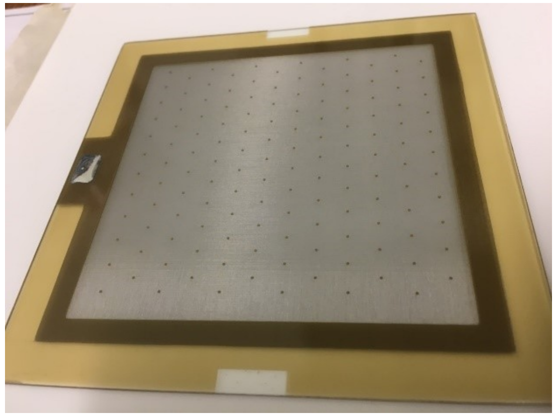

*Glass Micromegas*

# DETECTOR CHARACTERIZATION WITH X-RAYS (CERN GDD)

## X-ray radiography (20 kV) – Ar/$CF_4$(20%)

- High gain: 1 min exposure time gives images with good contrast

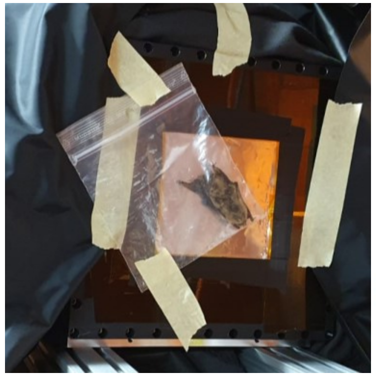

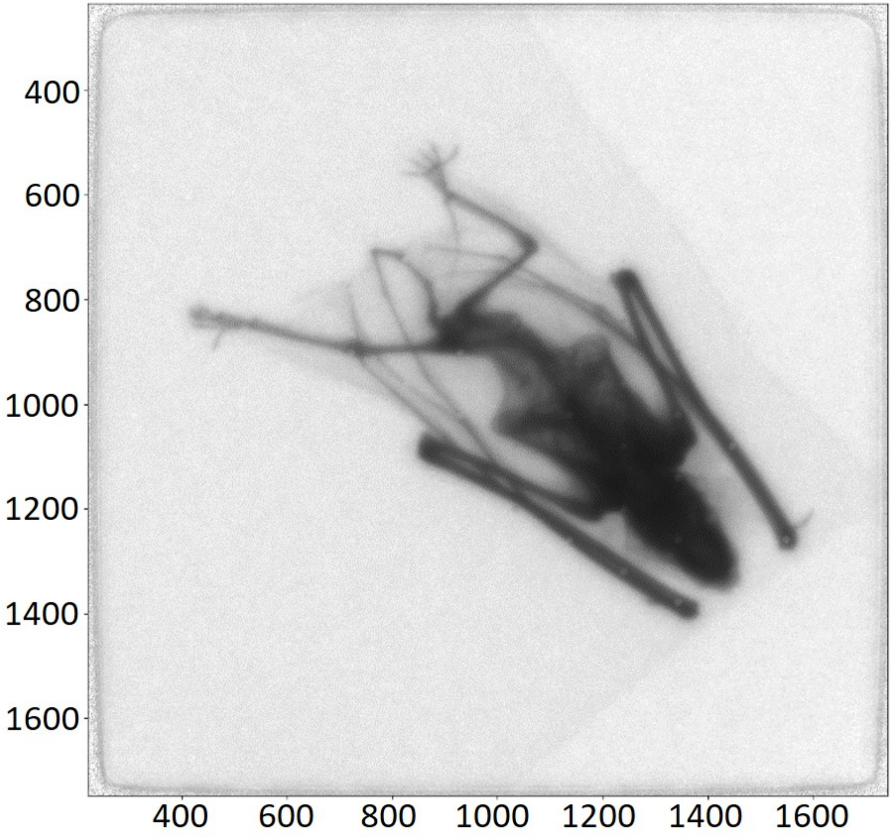


*60 sec exposure time bat radiography with simple background suppression and beam profile correction.*

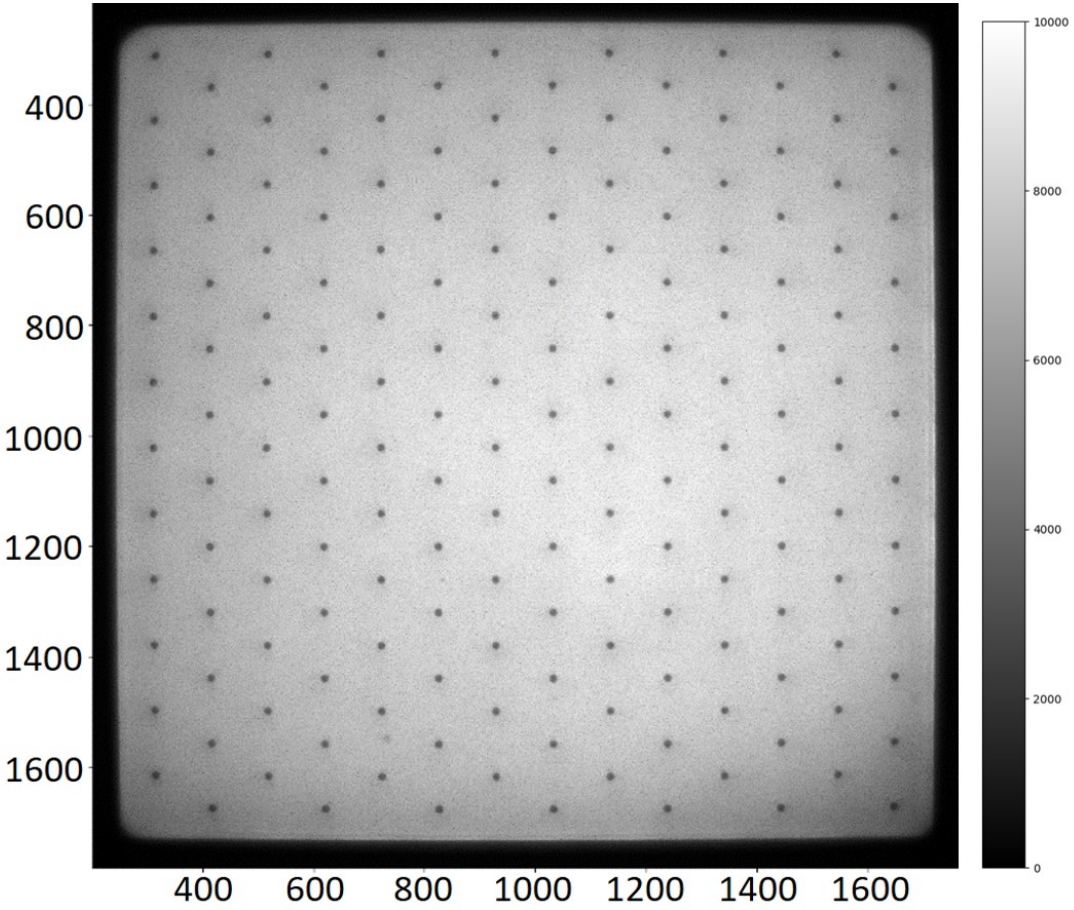


*60 sec full detector image with simple background suppression.*

# SOLEIL BEAM TEST (16/11-18/11)

## Synchrotron Soleil (4 keV – 15 keV)

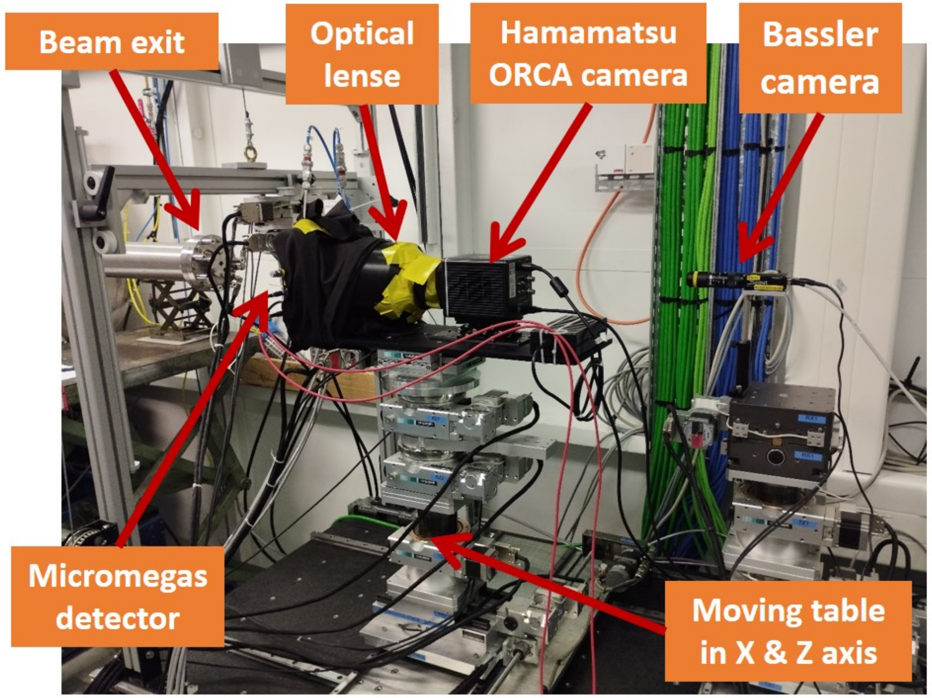


*Test of OPTIMED-BETA detector at hard X branch of METROLOGIE beamline*

## Goals

- Determination of Point Spread Function
- Spatial resolution dependence on drift gap, drift field and beam energy
- Detector homogeneity

PRELIMINARY

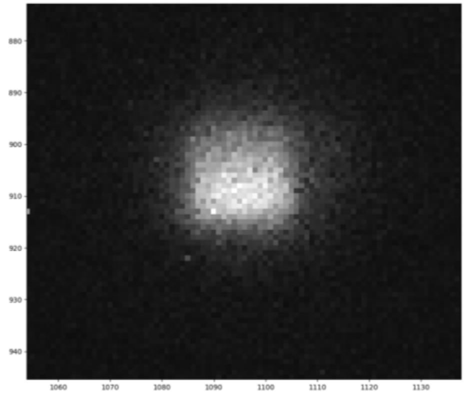

*1x1mm beam, Primary Scintillation (Va=0 V, Vd=0 V)*

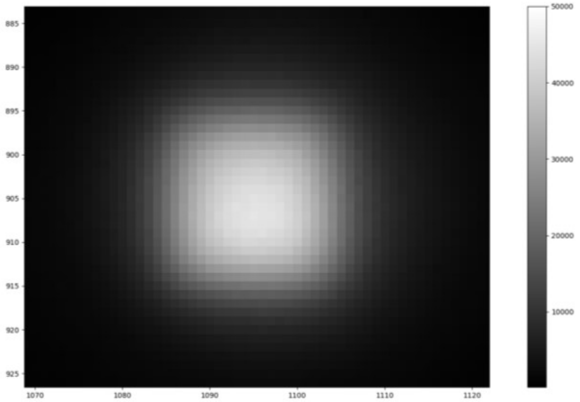

*1x1mm beam, Amplification (Va=400 V, Vd=210 V)*

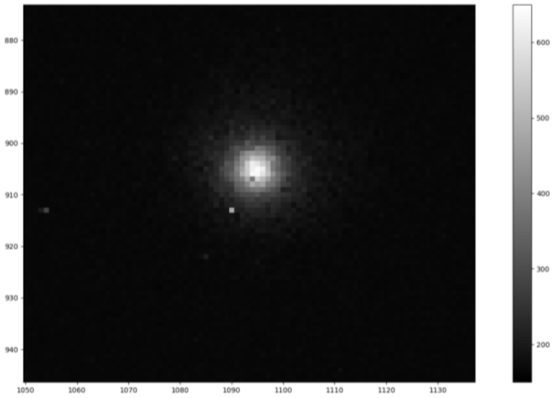

*0.035x0.035mm beam, Amplification (Va=400 V, Vd=210 V)*

*35 x 35 µm² beam, 6keV, Drift gap = 3 mm*

PRELIMINARY

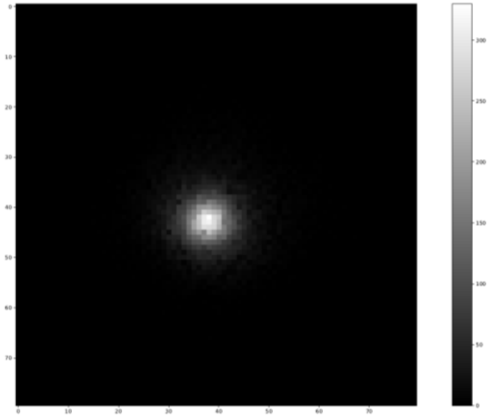

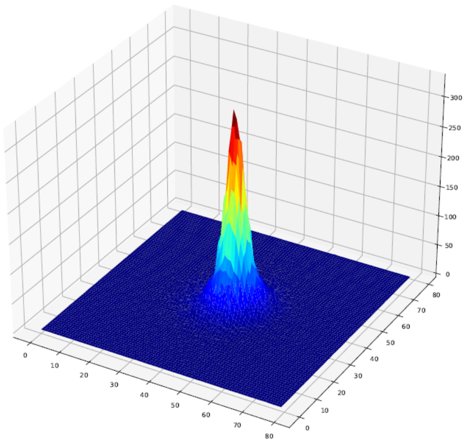

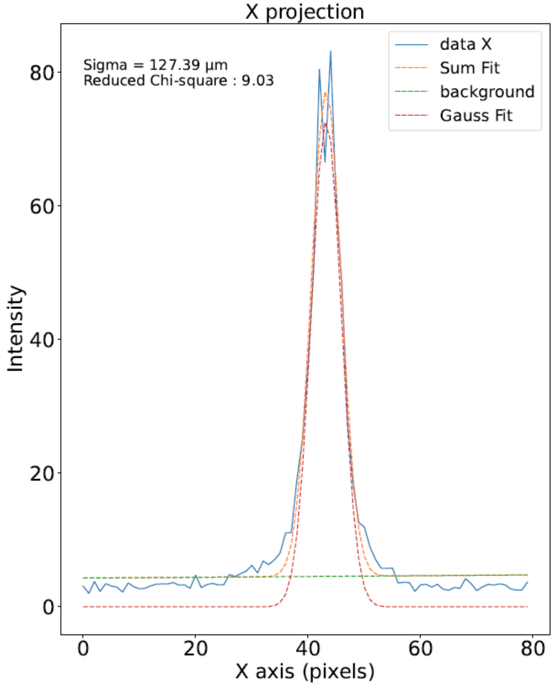


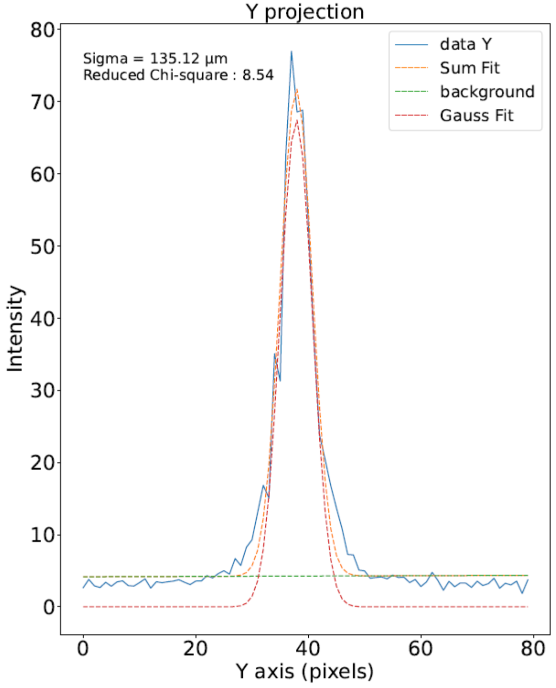


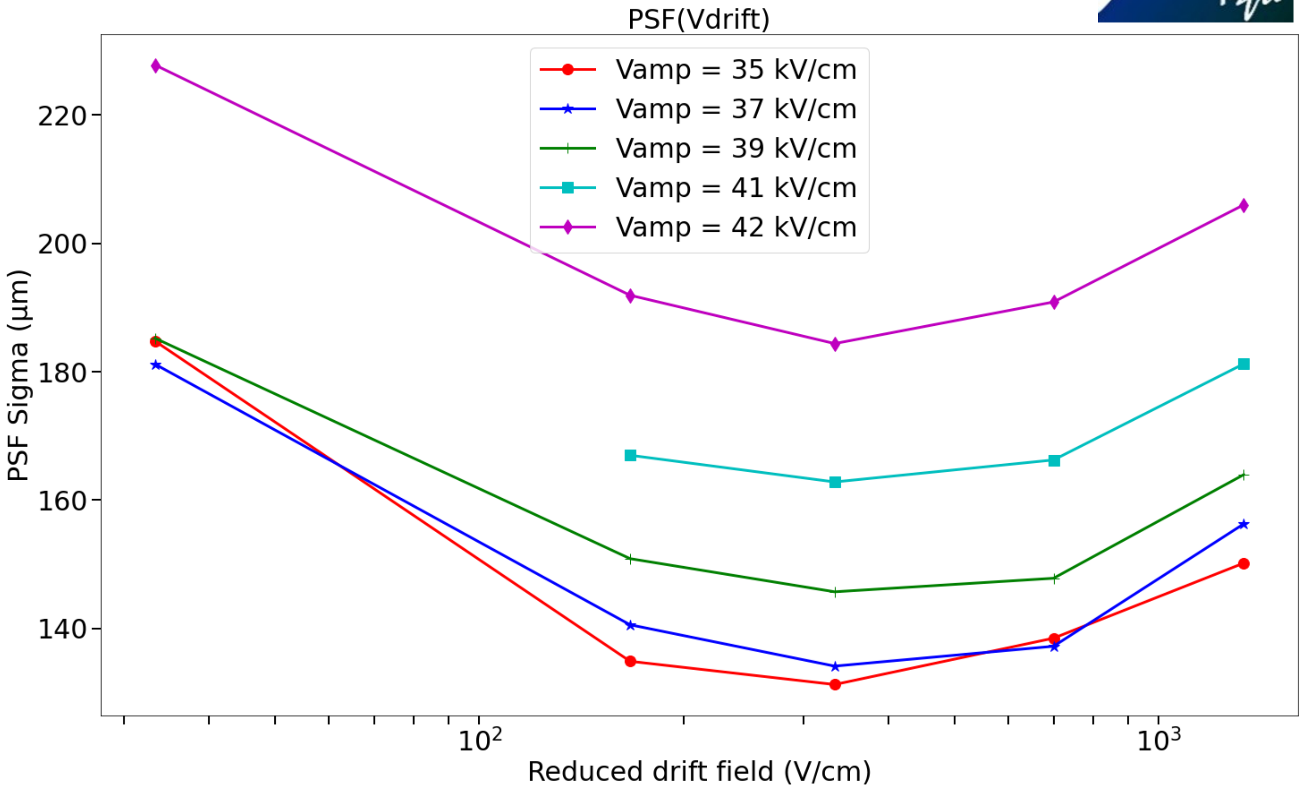


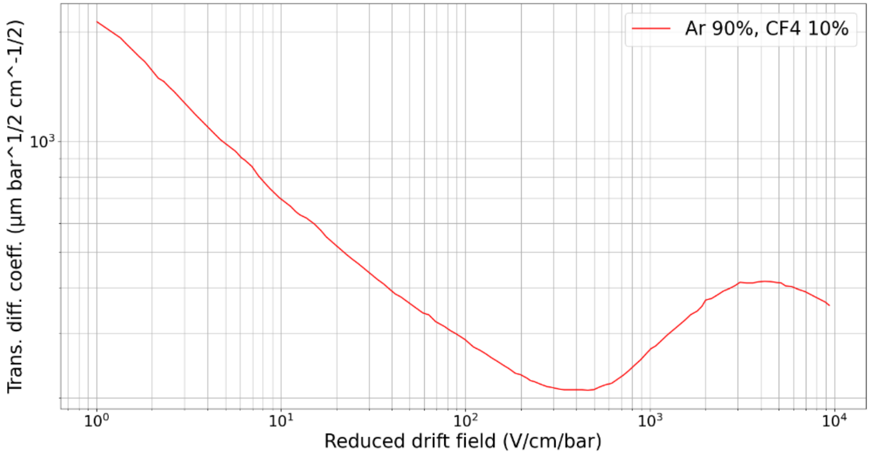


*Va=450 V, Vd=100 V*

## B-IMAGING

## PRELIMINARY RESULTS WITH TRITIUM SAMPLES

## NEUTRON RADIOGRAPHY

## PRELIMINARY RESULTS WITH A NEUTRON SOURCE

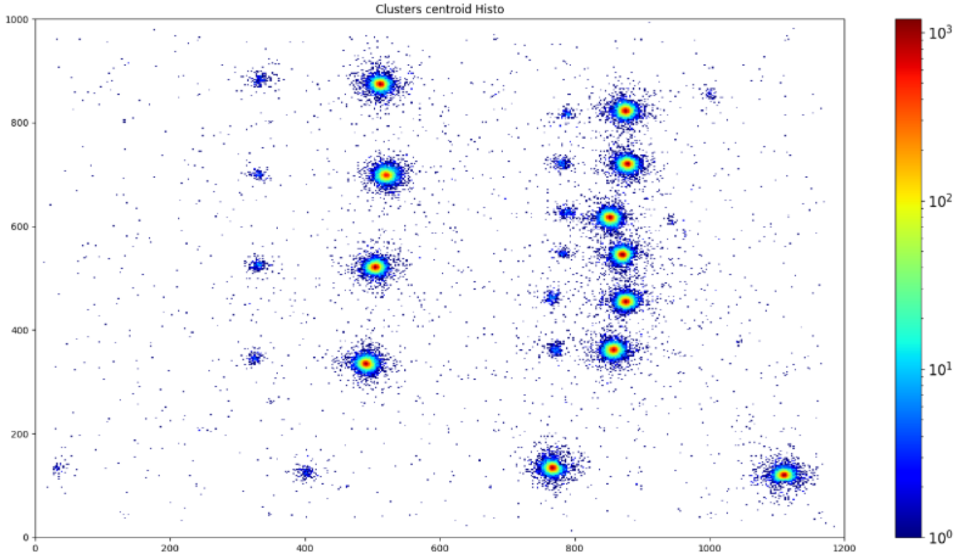


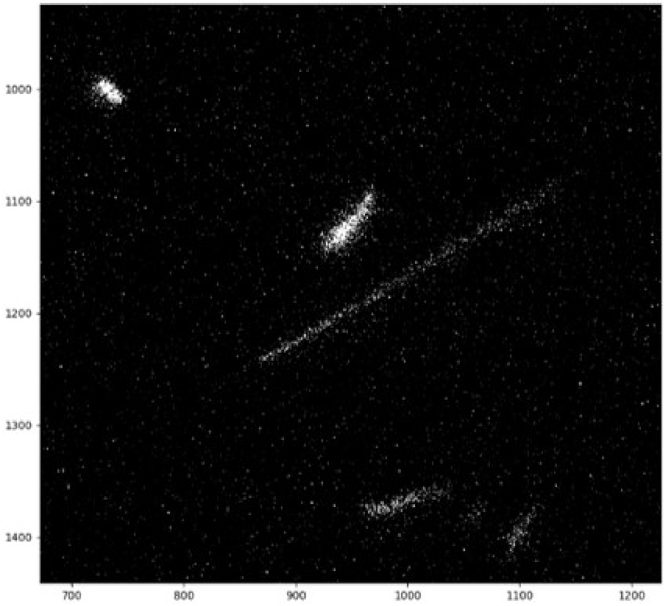

# B-IMAGING

## Tumor heterogeneity: different cell types inside a tumor

- Heterogeneity effect on drug targeting?
- Will help the developing of more efficient drugs
- Requires better detection sensibilities

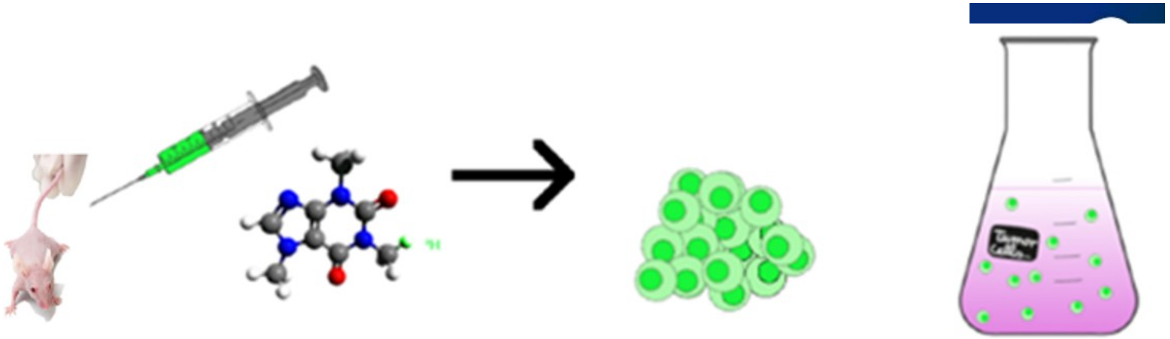

Tumoural cells collected from an animal – Tritium tracking

Cellular culture

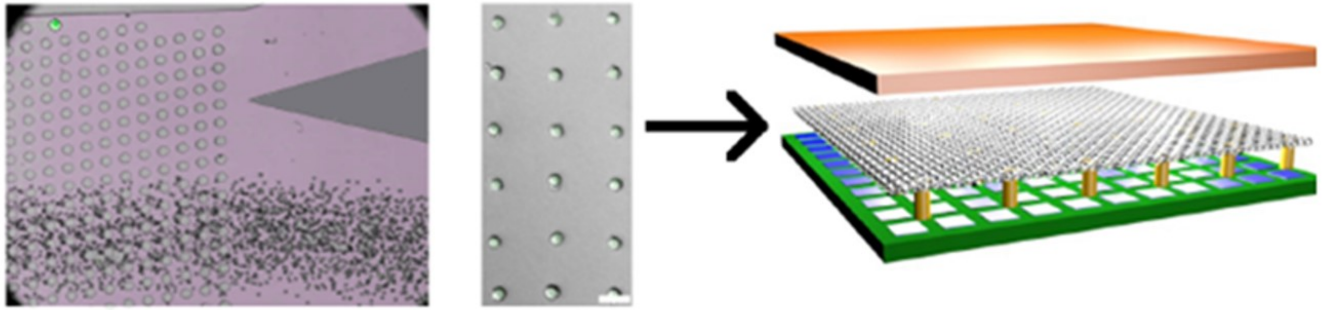

Cell deposit by microfluidics techniques

Tritium activity counting with gaseous detector

## <u>Molecule labelling and tracking with tritium</u>

Pharmaceutical needs at the cell level for drug development:

- Assess the **drug distribution** among cells
- Evaluate the impact of the cell heterogeneity on drug biodistribution
- At the cell level: Quantification of $^{3}$H concentration in **single cell** samples

# PRELIMINARY RESULTS WITH TRITIUM SAMPLES

## First deposit : tritiated glucose

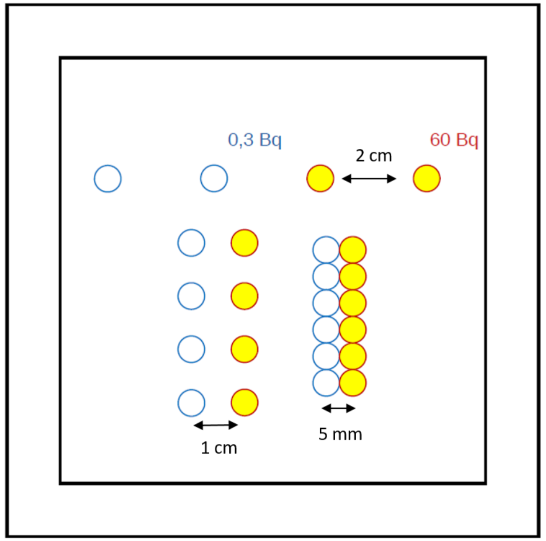


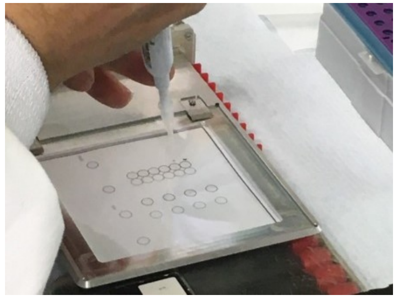

*Tritium deposits schema and picture*

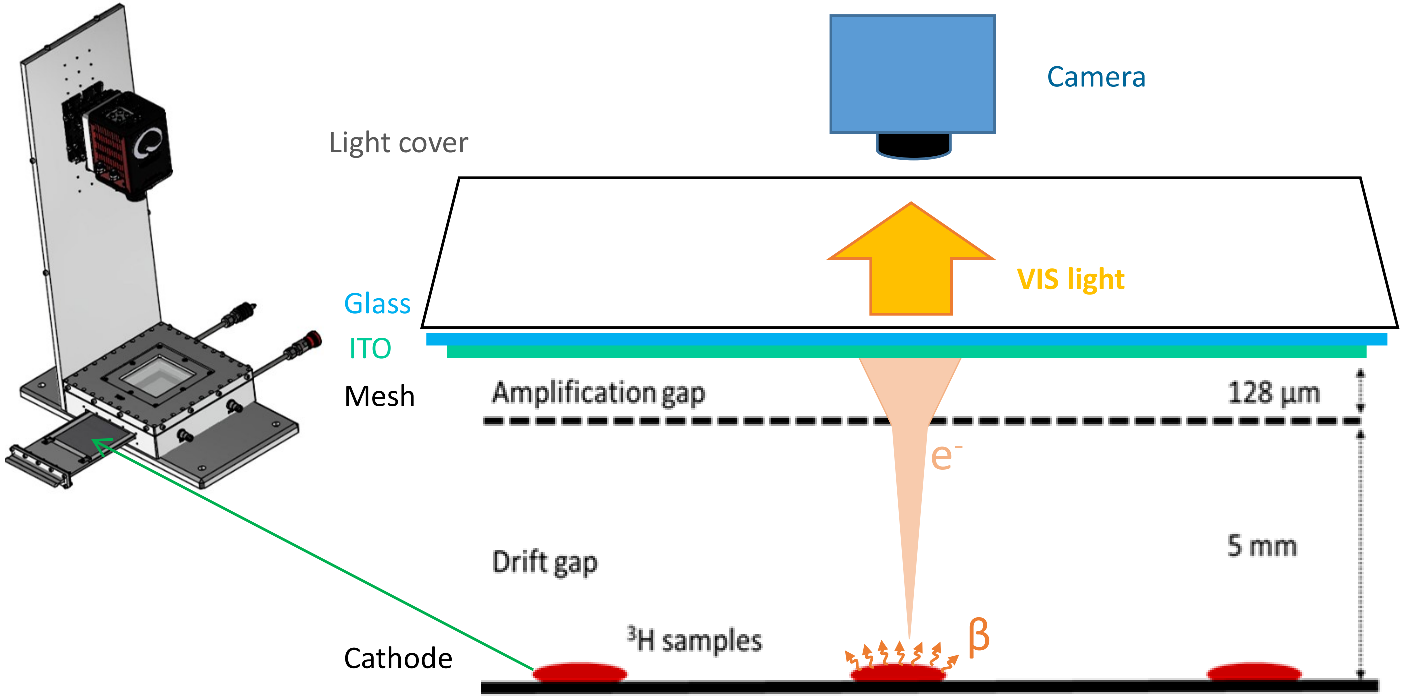


*OPTIMED-BETA set-up scheme*

- Activity measurement limits and dynamic range → Activities: 0.3 Bq and 60 Bq
- Spatial resolution → gap between drops: 2 cm – 1 cm – 5 mm

# PRELIMINARY RESULTS WITH TRITIUM SAMPLES

## Integration method :

- 60 Bq drops positions are well assessed
- 0.3 Bq drops hardly visible

*Light intensity profile*

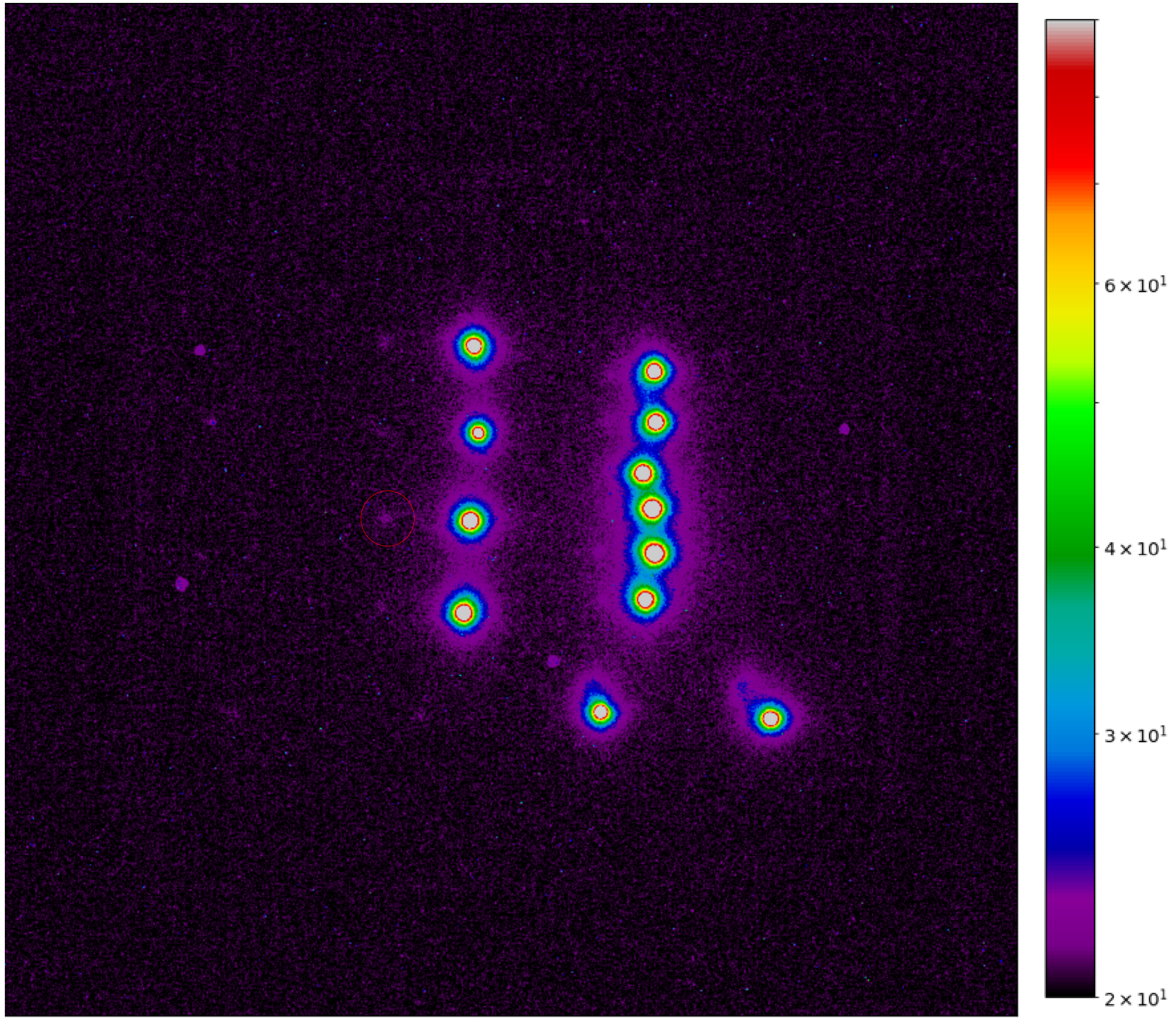


$Ar/CF_4(20\%)$

*180 frames of 10 sec (30 min) added with simple background suppression 20% of CF4*

# PRELIMINARY RESULTS WITH TRITIUM SAMPLES

## Clustering method :

*Clusters barycenter histogram*

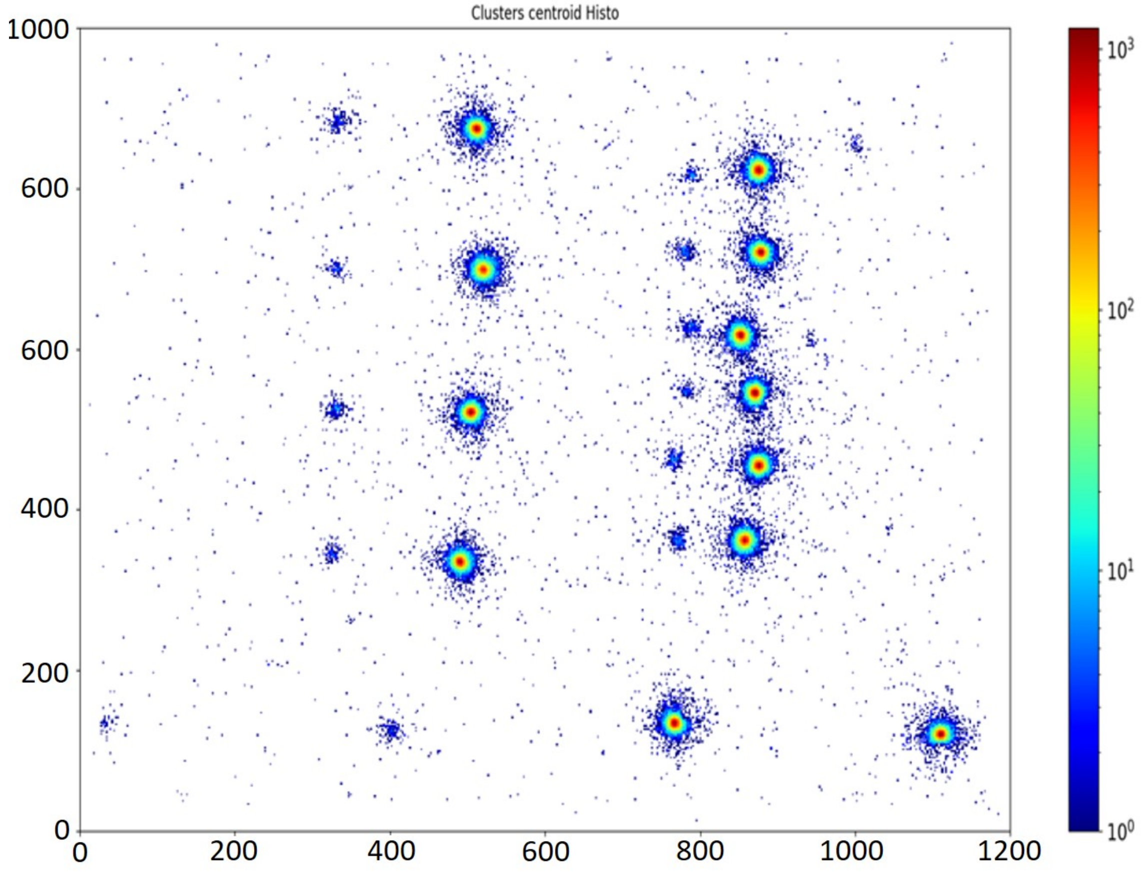


*20000 frames of 100 msec (33 min), individual pixel background thresholding, 20% of CF4*

- ➢ Both 60 Bq and 0.3 Bq drops positions are well assessed
- ➢ Better signal-to-noise ratio and counting events capability

# NEUTRON RADIOGRAPHY

## Micromegas-based neutron imager

$^{10}B_4C$ neutron-to-charge converter

- **Thermal neutrons** absorbed by 2 µm thin $^{10}B_4C$ layer
- Conversion efficiency: 5%
- (α or Li) fragments causes strong ionisation compared to electrons
- Drawback: fragments long range in the gas (5 mm)

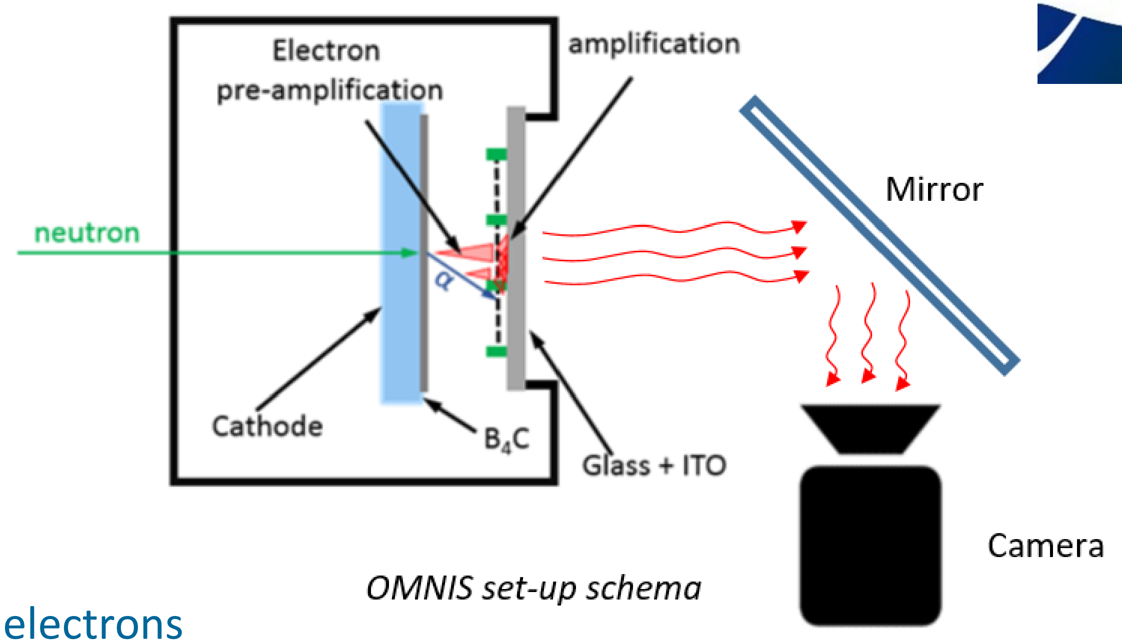


*OMNIS set-up schema*

Acquisition modes:

- **Event-by-event**: track reconstruction:

potentially higher resolution (100 µm), better ɣ-to-n suppression

- **Integrated**: real-time radiography:

ɣ-to-n suppression less efficient

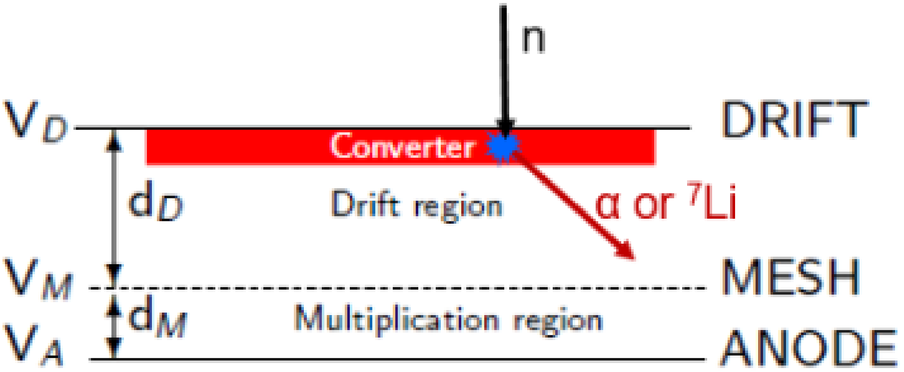


*Boron converter principle*

# PRELIMINARY RESULTS WITH A NEUTRON SOURCE

## Experimental set-up

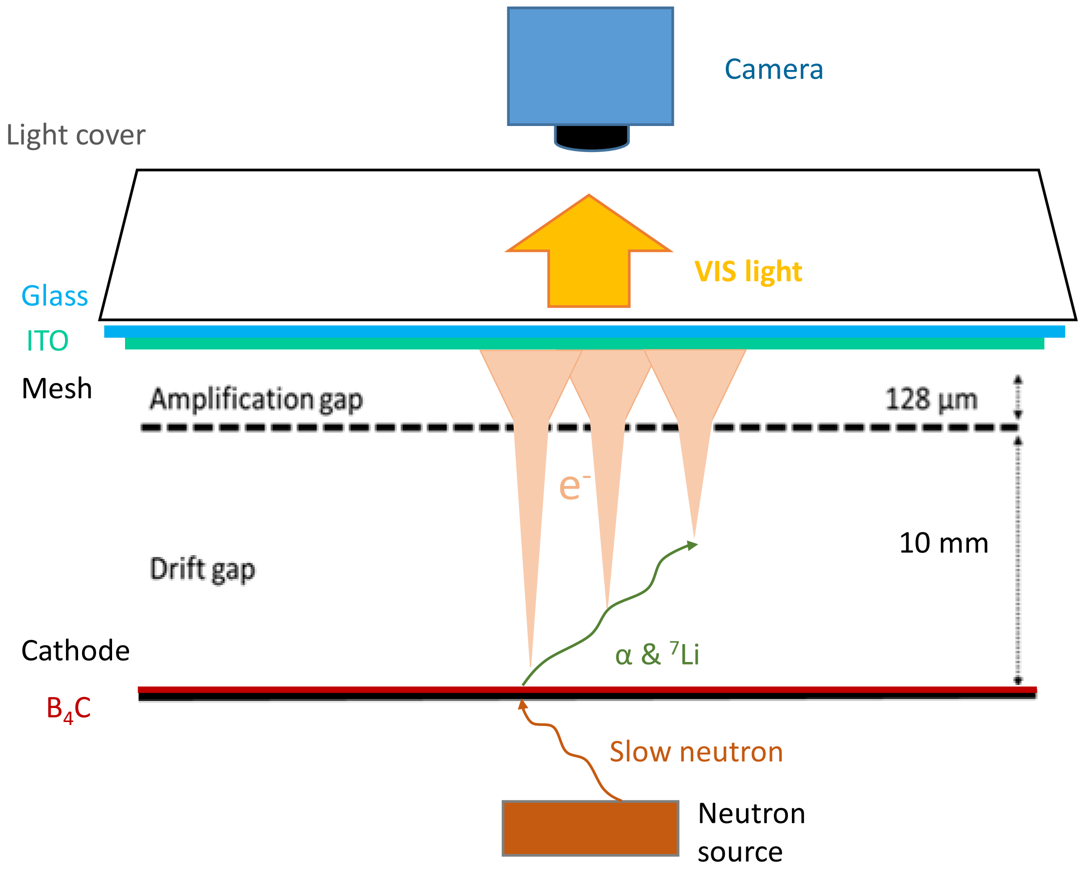


*OMNIS set-up schema*

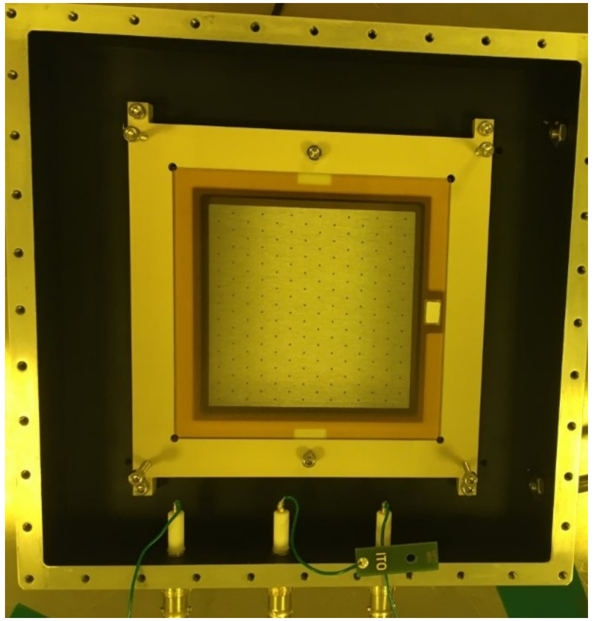

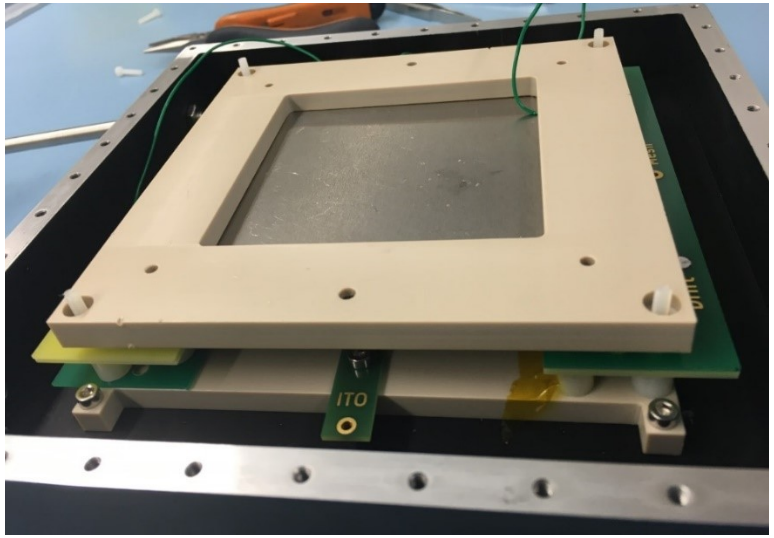

# PRELIMINARY RESULTS WITH A NEUTRON SOURCE (CERN GDD)

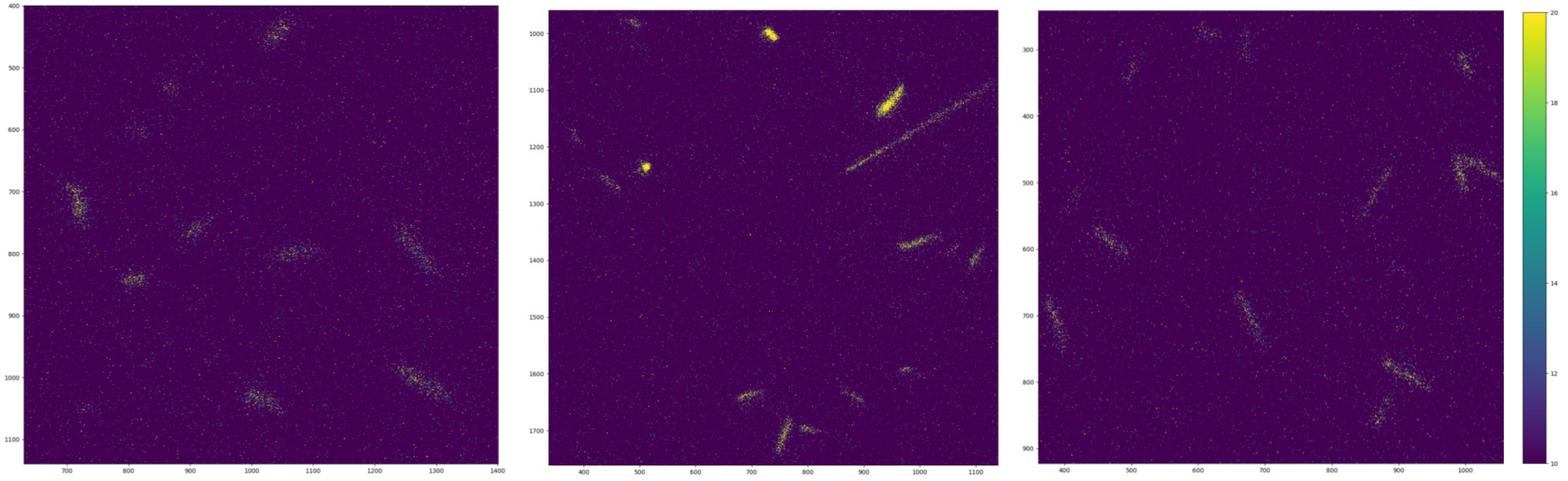

***50** V/cm drift field*

***800** V/cm drift field*

***2000** V/cm drift field*

*Transverse diffusion in 80% Argon + 20% CF4 gas mixture.*

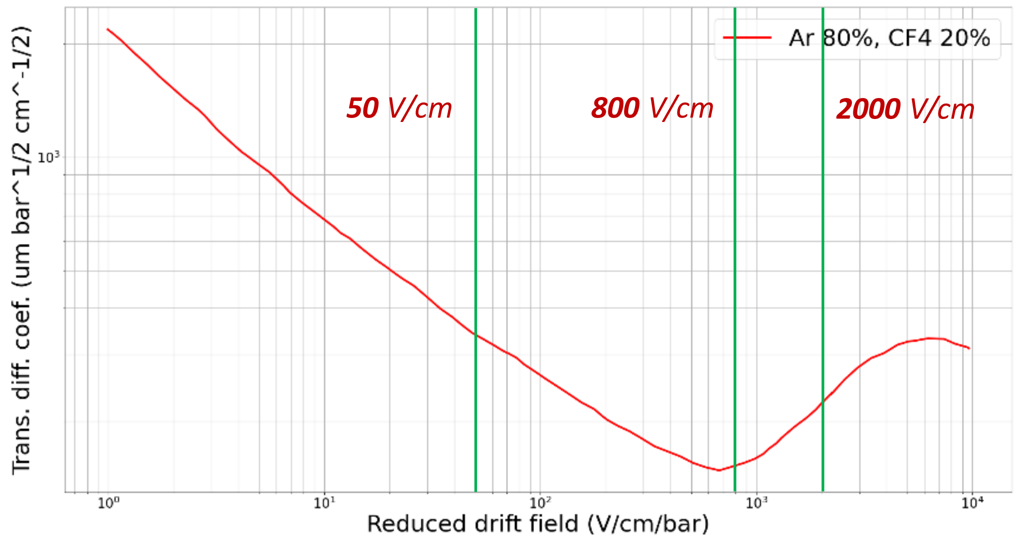


- Drift field affects the diffusion in the gas
- Diffusion spreads the light

PRELIMINARY

# CONCLUSION

## What we have done

- Several types of Micromegas on glass were built and tested
- Setups of optical readout detectors for neutron and beta detection
- Detector characterization at X-ray facilities, with beta samples and neutron sources
- Image processing in progress

## Outlook

- Beam test at Soleil accelerator: spatial resolution measurement and determination of point spread function
- Investigate image treatment methods
- β-imaging: tests on isolated single tumor cells
- Neutron radiography: Irradiation at neutron facilities

# THANK YOU

# BACK UP

# PRELIMINARY RESULTS WITH TRITIUM SAMPLES

## Clustering method :

*Charge readout coupling*

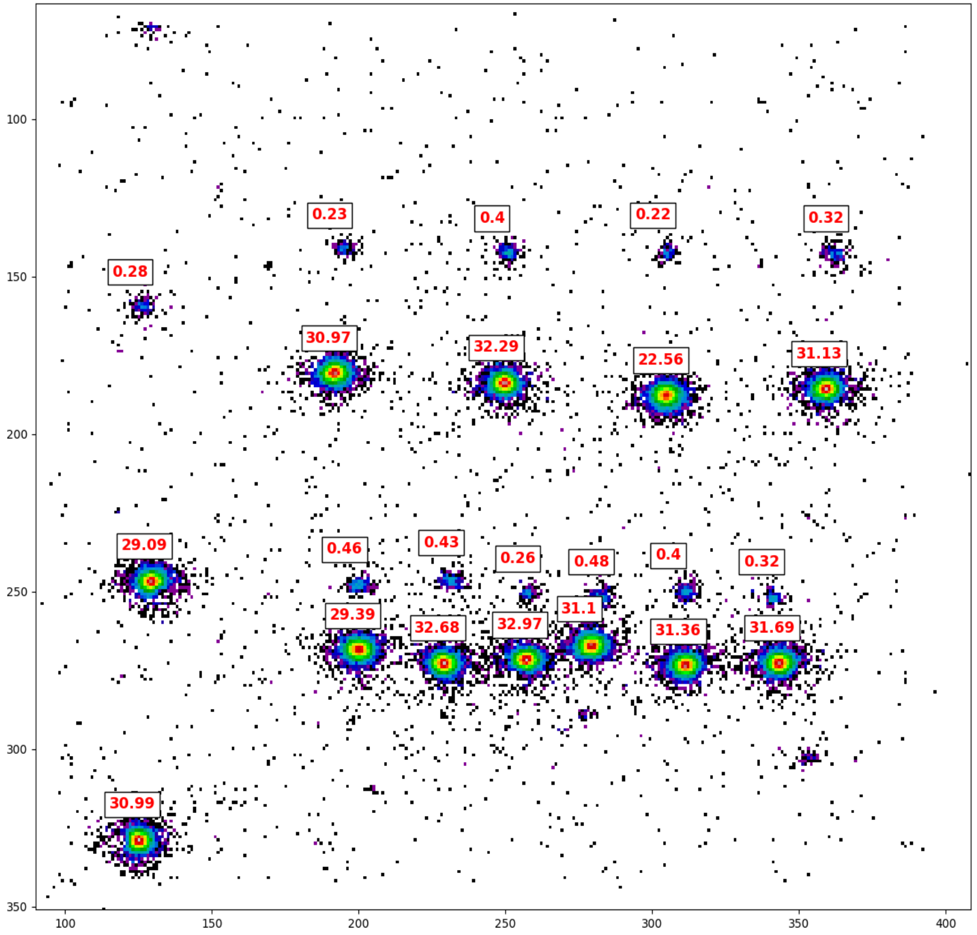


*Optical readout*

| | Mean activity (Bq) | Mean STD (Bq) |
|---|---|---|
| High activity | 8,4 | 0,74 |
| Low activity | 0,087 | 0,022 |

# Light production mechanisms

Scintillation : excited atoms or molecules emit photons during de-excitation.

**Scintillation**

- **Phosphorescence**
  Delayed emission of photons after absorption. (1 ms to 100 s)
- **Fluorescence**
  Prompt emission of photon after absorption of incident radiation. (1 ns to 1 µs)
  - **Primary scintillation**
    From the creation of primary electron coming from the excitation of gaz due to incident particles.
  - **Secondary scintillation**
    From the creation of secondary electrons taking place during avalanche amplification.
- **Electroluminescence**
  Electrons with energy lower than ionization threshold just excite atoms or molecules.

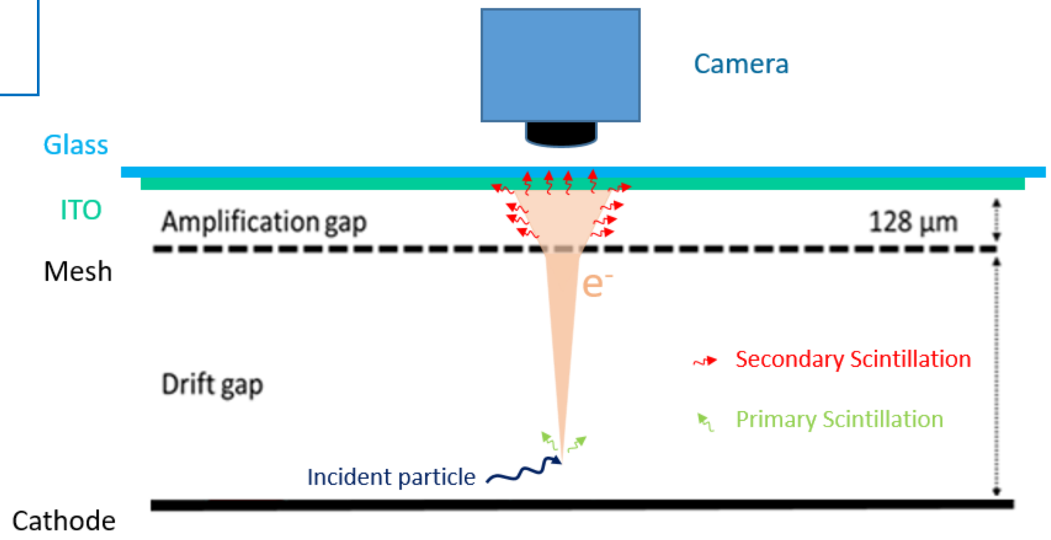


Light yield : amount of light determines the signal to noise ratio. It depends on electric field, pressure and gas mixture.

# PRELIMINARY RESULTS WITH TRITIUM SAMPLES

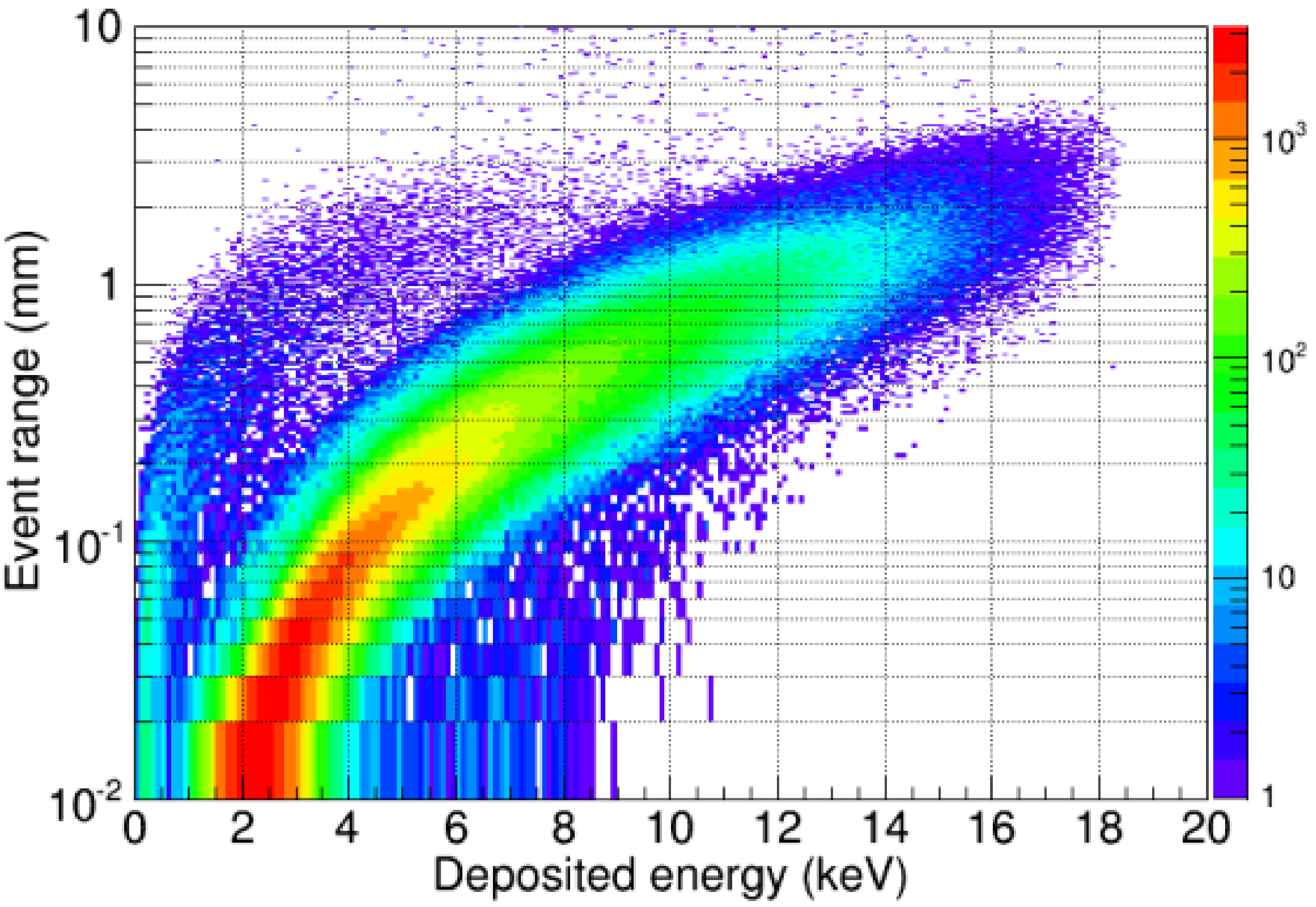


β particle range in Ar-Isobutane gas mixture

# DETECTOR CHARACTERIZATION WITH X-RAYS

## X-ray radiography

- MTF measurement

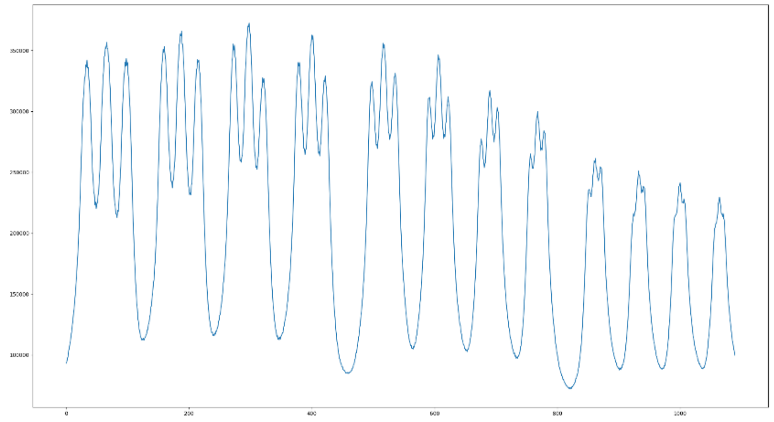

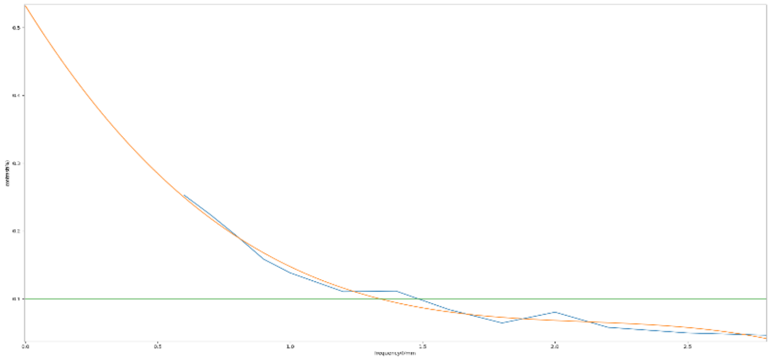

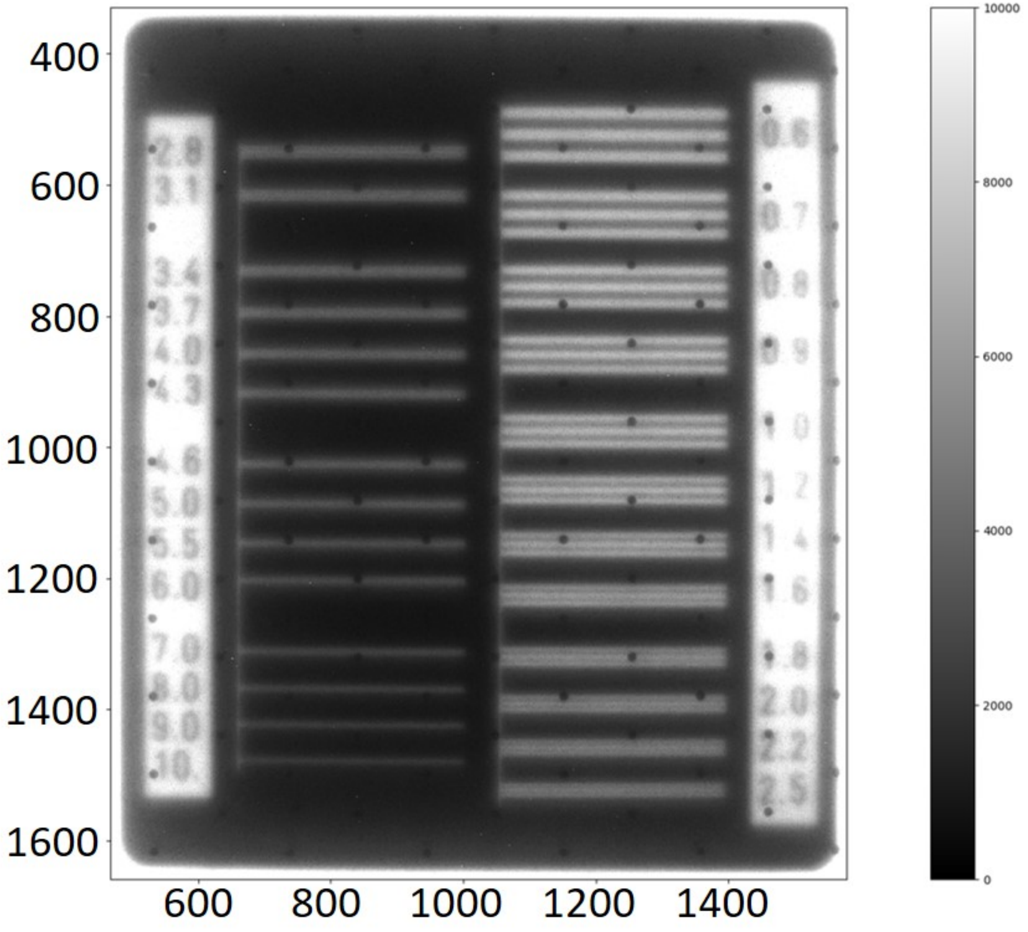


60 sec exposure time lead target radiography with simple background suppression.

# SOLEIL BEAM TEST (16/11-18/11)

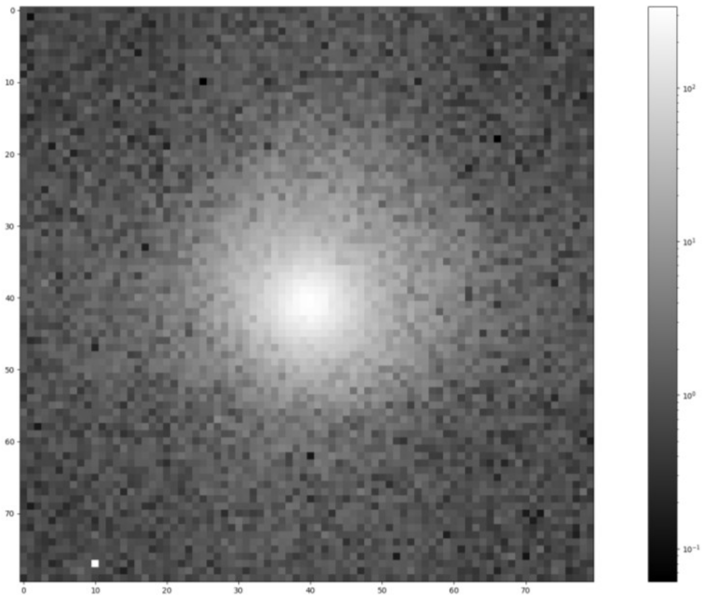

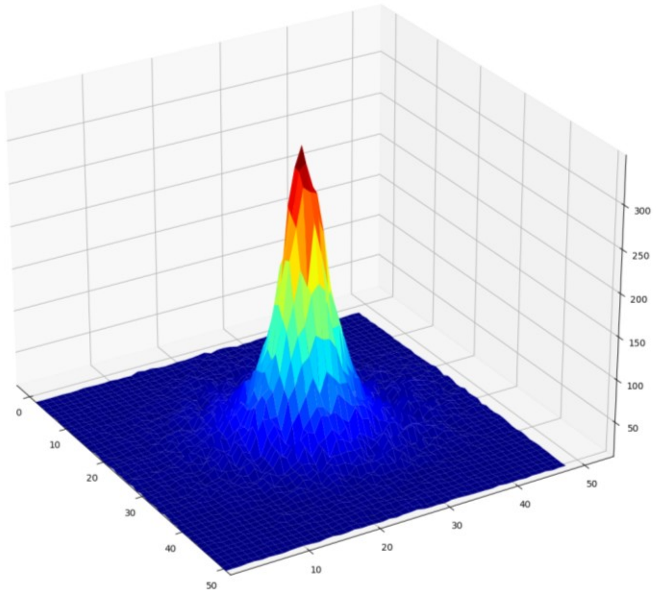

*Va=550 V, Vd=210 V*

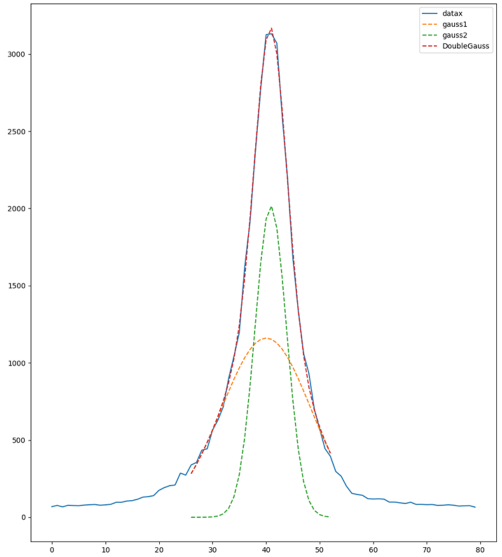


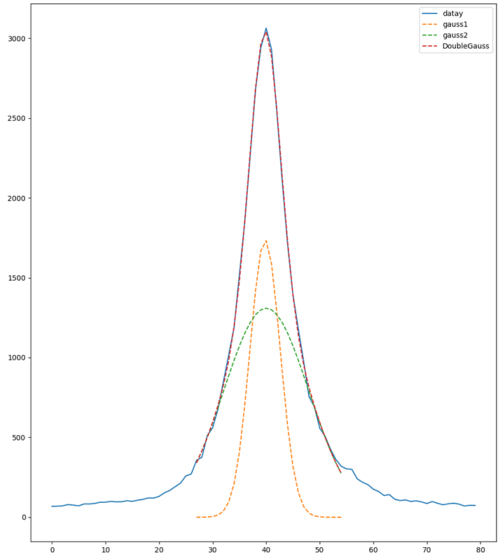


```
[[Fit Statistics]]
    # fitting method   = leastsq
    # function evals   = 1751
    # data points      = 27
    # variables        = 6
    chi-square         = 39420.8208
    reduced chi-square = 1877.18194
    Akaike info crit   = 208.727738
    Bayesian info crit = 216.502760
[[Variables]]
    g1_amplitude:  24252.9800 +/- 796.013491 (3.28%) (init = 3131.459)
    g1_center:     40.0220155 +/- 0.16008134 (0.40%) (init = 41)
    g1_sigma:      8.33708047 +/- 0.38782524 (4.65%) (init = 2)
    g1_fwhm:       19.6323238 +/- 0.91325863 (4.65%) == '2.3548200*g1_sigma'
    g1_height:     1160.54291 +/- 83.6092695 (7.20%) == '0.3989423*g1_amplitude/max(1e-15, g1_sigma)'
    g2_amplitude:  14893.5940 +/- 985.544332 (6.62%) (init = 3131.459)
    g2_center:     40.8678940 +/- 0.04921094 (0.12%) (init = 41)
    g2_sigma:      2.94535109 +/- 0.09062681 (3.08%) (init = 2)
    g2_fwhm:       6.93577165 +/- 0.21340982 (3.08%) == '2.3548200*g2_sigma'
    g2_height:     2017.30947 +/- 79.9626750 (3.96%) == '0.3989423*g2_amplitude/max(1e-15, g2_sigma)'
[[Correlations]] (unreported correlations are < 0.100)
    C(g2_amplitude, g2_sigma)     = 0.922
    C(g1_sigma, g2_amplitude)     = 0.894
    C(g1_amplitude, g2_amplitude) = -0.888
    C(g1_amplitude, g2_sigma)     = -0.862
    C(g1_sigma, g2_sigma)         = 0.755
    C(g1_amplitude, g1_sigma)     = -0.638
    C(g1_center, g2_center)       = -0.442
    C(g1_amplitude, g1_center)    = 0.357
    C(g1_center, g2_amplitude)    = -0.319
    C(g1_sigma, g2_center)        = -0.315
    C(g1_center, g2_sigma)        = -0.308
    C(g2_amplitude, g2_center)    = -0.233
    C(g1_center, g1_sigma)        = -0.195
    C(g2_center, g2_sigma)        = -0.186
    C(g1_amplitude, g2_center)    = 0.131
[[Fit Statistics]]
    # fitting method   = leastsq
    # function evals   = 123
    # data points      = 28
    # variables        = 6
    chi-square         = 20811.7844
    reduced chi-square = 945.990199
    Akaike info crit   = 197.109964
    Bayesian info crit = 205.103191
[[Variables]]
    g1_amplitude:  12274.5142 +/- 694.175066 (5.66%) (init = 3063.108)
    g1_center:     39.8013459 +/- 0.03745693 (0.09%) (init = 40)
    g1_sigma:      2.82109227 +/- 0.07424611 (2.63%) (init = 2)
    g1_fwhm:       6.64316450 +/- 0.17483622 (2.63%) == '2.3548200*g1_sigma'
    g1_height:     1735.78971 +/- 58.4831826 (3.37%) == '0.3989423*g1_amplitude/max(1e-15, g1_sigma)'
    g2_amplitude:  26006.5767 +/- 575.709827 (2.21%) (init = 3063.108)
    g2_center:     40.0064641 +/- 0.08773170 (0.22%) (init = 40)
    g2_sigma:      7.92542093 +/- 0.22378900 (2.82%) (init = 2)
    g2_fwhm:       18.6629397 +/- 0.52698281 (2.82%) == '2.3548200*g2_sigma'
    g2_height:     1309.09432 +/- 61.1708860 (4.67%) == '0.3989423*g2_amplitude/max(1e-15, g2_sigma)'
[[Correlations]] (unreported correlations are < 0.100)
```

# SOLEIL BEAM TEST (16/11-18/11)

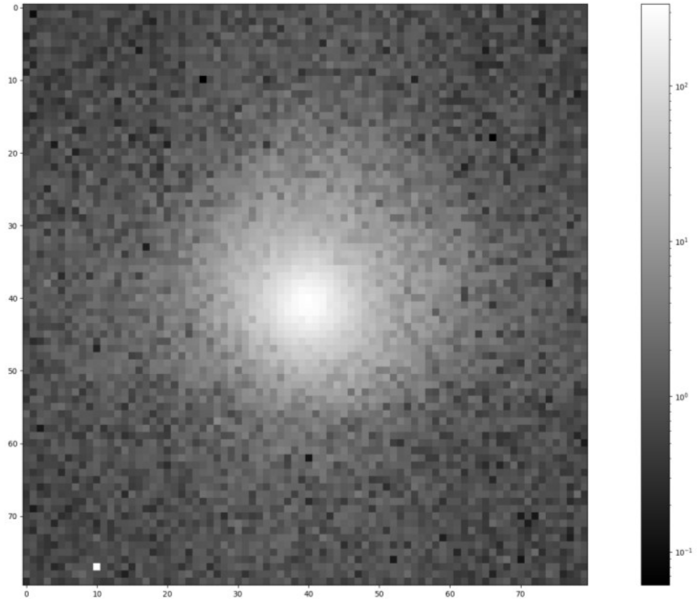


*Va=550 V, Vd=210 V*

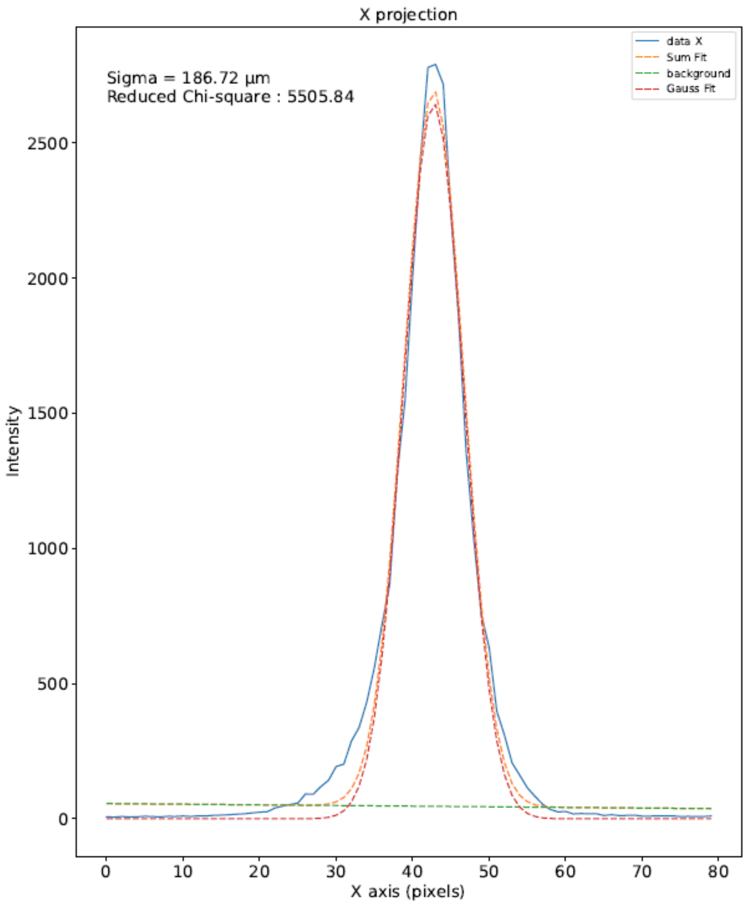


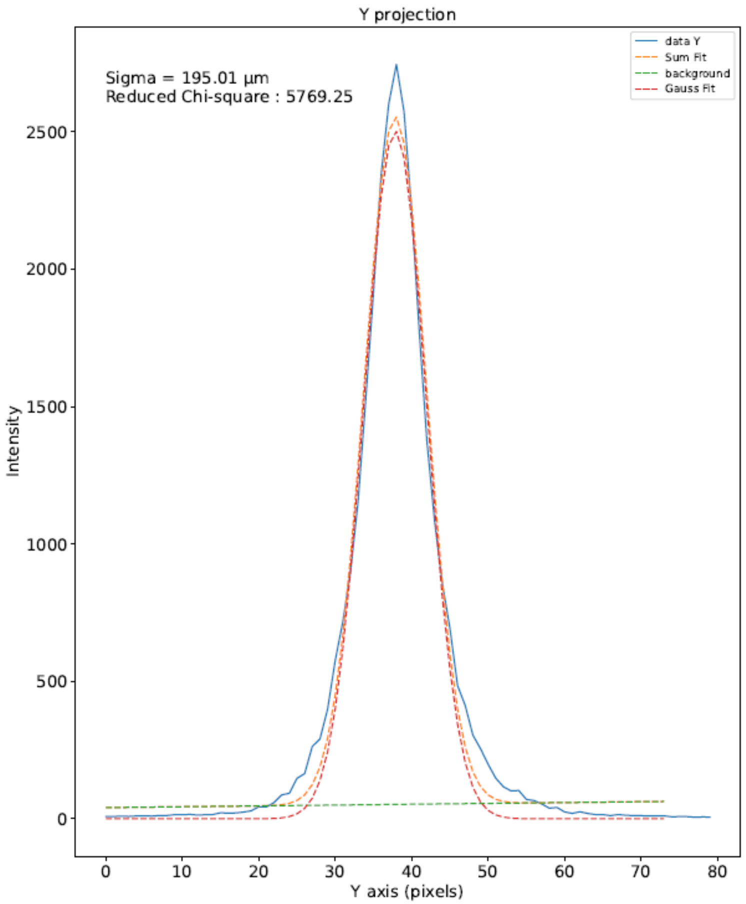

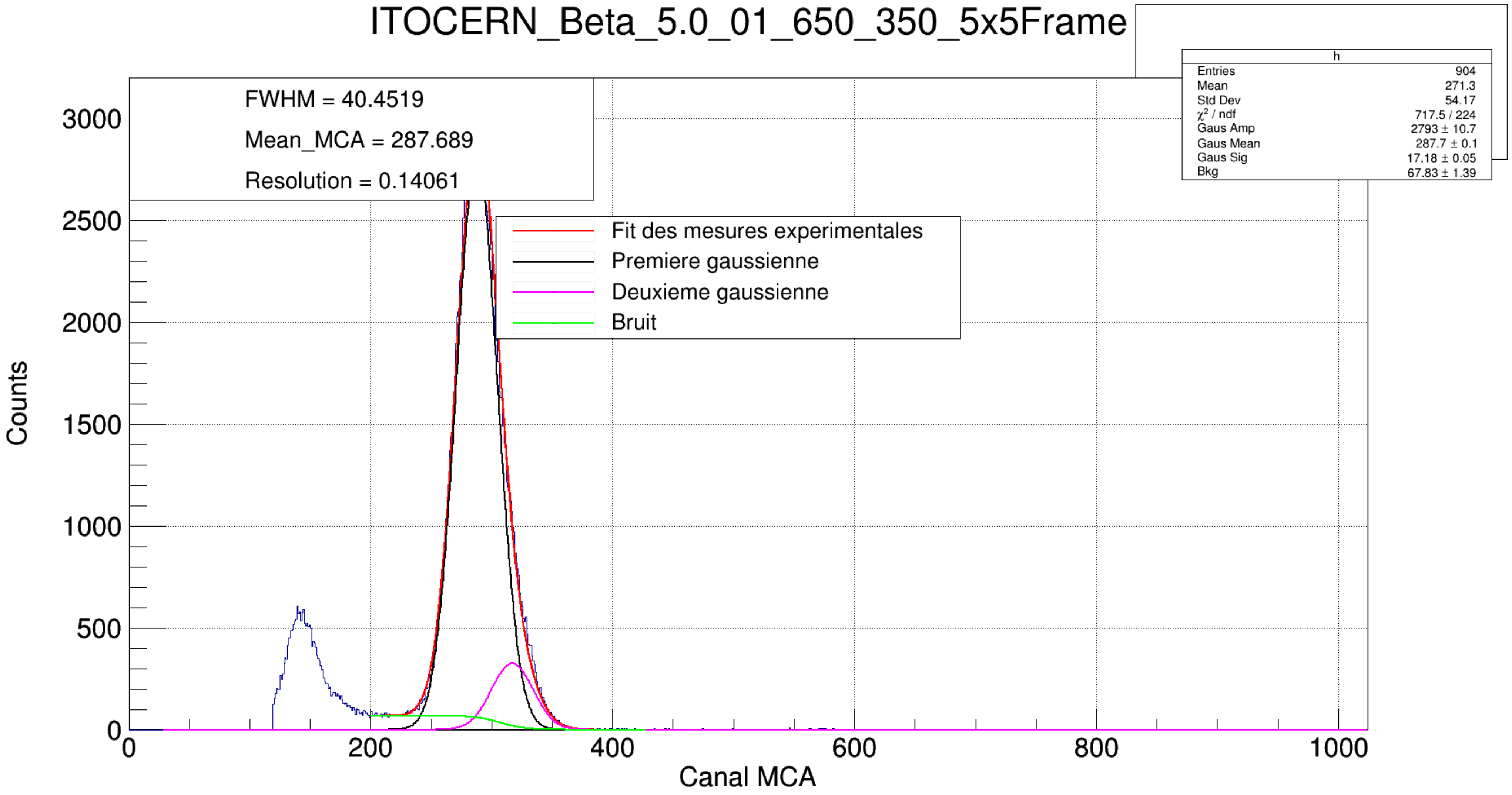
ITOCERN_Beta_5.0_01_650_350_5x5Frame
h
Entries 904
Mean 271.3
Std Dev 54.17
χ² / ndf 717.5 / 224
Gaus Amp 2793 ± 10.7
Gaus Mean 287.7 ± 0.1
Gaus Sig 17.18 ± 0.05
Bkg 67.83 ± 1.39
FWHM = 40.4519
Mean_MCA = 287.689
Resolution = 0.14061
Fit des mesures experimentales
Premiere gaussienne
Deuxieme gaussienne
Bruit
Counts
Canal MCA
0
500
1000
1500
2000
2500
3000
200
400
600
800
1000

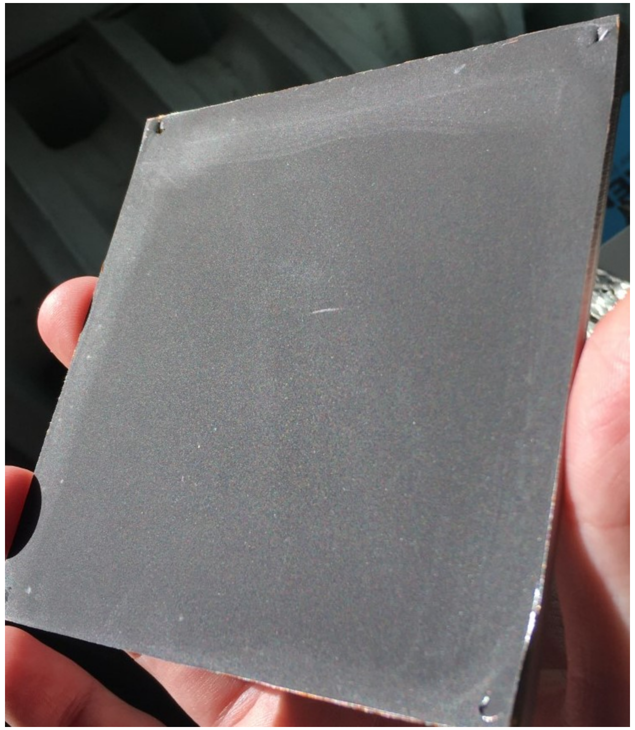

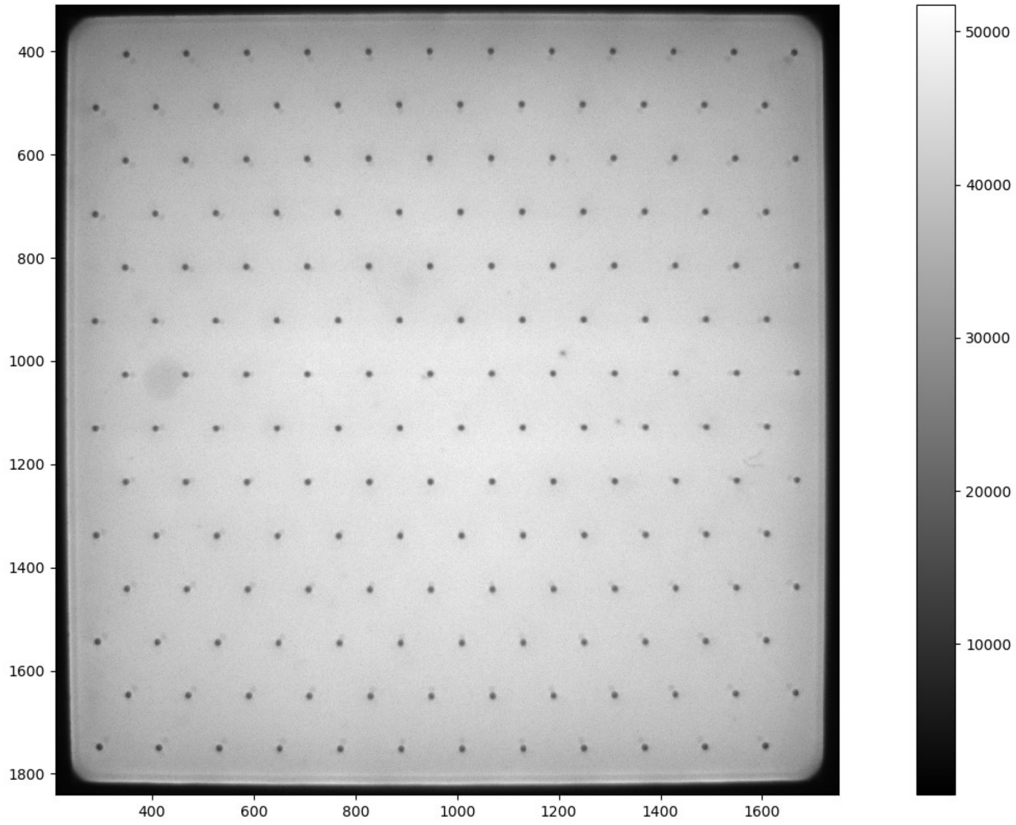
400
600
800
1000
1200
1400
1600
1800
400
600
800
1000
1200
1400
1600
50000
40000
30000
20000
10000